International Journal of Psychophysiology 130 (2018) 9–20

Contents lists available at ScienceDirect

International Journal of Psychophysiology

journal homepage: www.elsevier.com/locate/ijpsycho

Junior temperament character inventory together with quantitative EEG discriminate children with attention deficit hyperactivity disorder combined subtype from children with attention deficit hyperactivity disorder combined subtype plus oppositional defiant disorder

Giuseppe A. Chiarenza[a,b,*], Stefania Villa[b], Lidice Galan[c,e], Pedro Valdes-Sosa[c,e], Jorge Bosch-Bayard[d,**]

[a] Centro Internazionale dei Disturbi di Apprendimento, Attenzione e Iperattività, (CIDAAI), Milano, Italy
[b] Unità Operativa di Neuropsichiatria Infantile, ASST Rhodense, Rho, Milano, Italy
[c] The Clinical Hospital of Chengdu Brain Science Institute, MOE Key Lab for Neuroinformation, University of Electronic Science and Technology of China, Chengdu, China
[d] Institute of Neurobiology, UNAM, Mexico
[e] Cuban Neuroscience Center, Havana, Cuba

ARTICLE INFO

Keywords:
ADHD_C, ODD
qEEG
qEEGT
Source localization
JTCI
Temperament
Character

ABSTRACT

Oppositional defiant disorder (ODD) is frequently associated with Attention Deficit Hyperactivity Disorder (ADHD) but no clear neurophysiological evidence exists that distinguishes the two groups. Our aim was to identify biomarkers that distinguish children with Attention Deficit Hyperactivity Disorder combined subtype (ADHD_C) from children with ADHD_C + ODD, by combining the results of quantitative EEG (qEEG) and the Junior Temperament Character Inventory (JTCI).

28 ADHD_C and 22 ADHD_C + ODD children who met the DSMV criteria participated in the study. JTCI and EEG were analyzed. Stability based Biomarkers identification methodology was applied to the JTCI and the qEEG separately and combined. The qEEG was tested at the scalp and the sources levels. The classification power of the selected biomarkers was tested with a robust ROC technique. The best discriminant power was obtained when TCI and qEEG were analyzed together. Novelty seeking, self-directedness and cooperativeness were selected as biomarkers together with F4 and Cz in Delta; Fz and F4 in Theta and F7 and F8 in Beta, with a robust AUC of 0.95 for the ROC. At sources level: the regions were the right lateral and medial orbito-frontal cortex, cingular region, angular gyrus, right inferior occipital gyrus, occipital pole and the left insula in Theta, Alpha and Beta. The robust estimate of the total AUC was 0.91. These structures are part of extensive networks of novelty seeking, self-directedness and cooperativeness systems that seem dysregulated in these children. These methods represent an original approach to associate differences of personality and behavior to specific neuronal systems and subsystems.

1. Introduction

Oppositional defiant disorder (ODD) and Attention Deficit Hyperactivity Disorder combined subtype (ADHD_C) are developmental disorders that are among the most commonly diagnosed mental health conditions in childhood (Hamilton and Armando, 2008; Loeber et al., 2009). Community samples show a prevalence rate for ODD ranging between 2 and 14% (Boylan et al., 2007; Loeber et al., 2000). ODD is more prevalent in boys than in girls with ratio's ranging from 3:1 to 9:1 prior to adolescence (Loeber et al., 2000). ODD is a condition involving problems in self-control of emotions and behaviors. The essential features are frequent and persistent pattern of angry/irritable mood, argumentative/defiant behavior, or vindictiveness (American Psychiatric Association, 2013). The disturbance in behavior is associated with distress in the individual or others in his or her immediate social context or it impacts negatively on social, educational, or other important areas of functioning. Neurocognitive impairments associated with ODD include lower IQ, deficiencies in inhibitory control, abnormalities in emotional processing and social cognition, and abnormalities in reinforcement processing. These impairments are thought to be related to

* Correspondence to: G.A. Chiarenza, Centro Internazionale dei disturbi di apprendimento, attenzione e iperattività, (CIDAAI), Milano, Italy.
** Corresponding author.
E-mail addresses: giuseppe.chiarenza@fastwebnet.it (G.A. Chiarenza), oldgandalf@gmail.com (J. Bosch-Bayard).

https://doi.org/10.1016/j.ijpsycho.2018.05.007
Received 13 February 2018; Received in revised form 28 April 2018; Accepted 18 May 2018
Available online 19 May 2018
0167-8760/

abnormalities in underlying brain mechanisms. Noordermeer et al. (2016) in a systematic review and meta-analysis of neuroimaging studies in children with ODD/CD, reported evidence of smaller brain structures and lower brain activity in the following areas: bilateral amygdala, bilateral insula, right striatum, left medial/superior frontal gyrus, and left precuneus. Similar evidence was found by Calzada-Reyes et al. (2016) in adolescents with ODD and in young adults with conduct disorder using quantified electroencephalogram (qEEG). The authors reported a pattern of beta activity excess with a peak at 17.1 Hz on bilateral fronto-temporo-striatal regions and alpha band power decrease on left central-temporal and right fronto-central-temporal regions.

One of the most frequent comorbidity associated to ODD is ADHD. The MTA study reports a frequency of 39,9% superior to anxiety disorder (34%) and conduct disorder (14%) (MTA, 1999). The essential feature of ADHD is a persistent pattern of inattention and/or hyperactivity that interferes with functioning or development and causes impairment in multiple settings: home, school and work. Population surveys suggest that in most cultures ADHD occurs in about 5% of children (Szatmari, 1992). One of the most cited model of ADHD_C is the one proposed by Barkley (1997a, 1997b, 1997c, 2006) which describes ADHD_C as a deficit in behavioral inhibition of four executive neuropsychological functions: working memory, self-regulation of affect–motivation–arousal, internalization of speech and reconstruction. Extensive neuroimaging studies (ERPs, PET, fMRI) have demonstrated that during the execution of cognitive tasks, children with ADHD show a pattern of hypoactivation of the prefrontal lobes and of the striatal regions. (Cortese et al., 2012; di Michele et al., 2005; Castellanos et al., 1994, 1996; Lou et al., 1984, 1989; Rubia et al., 1999, 2001, 2011; Hastings and Barkley, 1978; Klorman, 1992; Taylor, 1986). Neurophysiological studies have shown that different EEG patterns exist in ADHD children. The most frequent EEG patterns consist of elevated high amplitude theta with deficit or excess of beta activity and reduced alpha activity. This profile has been found primarily in children with the combined type of ADHD (Chabot et al., 1996, 2001; Clarke et al., 2001). Several studies have been conducted to associate these neurophysiological patterns with the diverse and multiform comorbidities present in ADHD subjects (Barry et al., 2003, Chabot et al., 2015). Although ADHD_C and ODD seem to share some similarities at neurofunctional level, Barry and Clarke (2009) and Clarke et al. (2002) found little EEG difference between groups of children with ADHD, with and without ODD. Their comment on this finding was: “considering the widespread occurrence of such comorbid disorders in school-age children, it is surprising how little reliable data are available on their EEG correlates. Further work is required to establish unique EEG signatures for such disorders and to resolve how they interact with the EEG deviations associated with ADHD itself.” On the other hand, Jaworska et al. (2013) examining qEEG relationships between anger and non-angry adults with ADHD noted increased beta1 associated with anger and it was interpreted as modest resting cortical hyperarousal.

To clinically assess the temperament and character of the children we used the Italian version (Andriola et al., 2012) of the Junior Temperament Character Inventory (JTCI) of Cloninger (Cloninger et al., 1993). The reason for this choice was that this is the only scale that has been translated into Italian and validated on a population of 459 subjects ranging in age from 6 to 15.9 years. The JTCI scale implements a psychobiological model in which personality is composed of temperament and character traits. In this model, temperament is defined as those aspects of personality that are emotion-based, moderately heritable, developmentally stable regardless of social and cultural influences (Cloninger et al., 1994; Cloninger and Svrakic, 2000). Four dimensions of temperament have been identified: 1) harm avoidance (HA, anxiety prone vs risk taking), 2) novelty seeking (NS, impulsive vs rigid), 3) reward dependence (RD, sociable vs aloof), 4) persistence (PS, persevering vs easily discouraged). Neuroimaging studies with SPECT and fMRI have identified the neural systems that underlie these dimensions. Novelty-seeking dimension is hypothesized to be regulated by the amygdaloid subdivision of the limbic system which receives sensory input through the orbital prefrontal network (MacLean, 1958, 1990; Kelly et al., 1973; Kelly, 1980) while persistence is associated with specific areas of the lateral orbital and medial prefrontal cortex and ventral striatum Gusnard et al., 2003). These basic emotional drives of temperament are regulated by 3 dimensions of character considered in terms of higher cognitive functions that regulate an individual's goal, values and mental self-government: 1) Self-Directedness (SD) expresses the individual's competence toward autonomy, reliability, and maturity 2) Cooperativeness (CO) is the ability to get along with other people by being tolerant, empathic, helpful, and forgiving, 3) Self-Transcendence (ST) is a person's ability to identify with nature and the world as a whole as a person seeks to understand what is beyond their individual human existence and is able to sublimate and act altruistically.

These seven TCI personality factors seem to be biologically distinct because each dimension has a unique genetic cause (Gillespie et al., 2003), a unique role in information processing (Cloninger, 2004) and a specific brain circuitry (Cloninger, 2002). Neuroimaging studies with SPECT and fMRI have identified the neural systems that underlie these dimensions. Cloninger has described the functional neuroanatomy of the four dimensions of temperament and how they are related to specific subdivisions of the limbic system (Cloninger, 2002). Therefore, harm avoidance is hypothesized to be a behavioral manifestation of individual differences in the septal subdivision of the limbic system regulating the tonic opposition of sexual drive necessary for reproduction versus the preservation of personal safety (MacLean, 1958, 1962, 1990). Individuals with high scores on HA show reduced white matter structural integrity in distributed brain areas, including corticolimbic pathways involved in emotional processing and reappraisal (Westlye et al., 2011). Furthermore, a significant negative correlation between scores on HA and gray matter volume was found in the right cuneus and inferior parietal lobule, in the left precuneus, middle occipital gyrus and middle frontal gyrus and bilaterally in the inferior frontal gyrus of normal subjects (Gardini et al., 2009). The novelty-seeking dimension is hypothesized to be regulated by the amygdaloid subdivision of the limbic system which receives sensory input through the orbital prefrontal network (MacLean, 1958, 1990; Kelly et al., 1973; Kelly, 1980). Significant positive correlations were observed between scores on novelty seeking and cerebral blood flow in the left anterior cingulate and in the right anterior and posterior insula (Sugiura et al., 2000). Recently, a significant positive correlation between scores on NS and gray matter volume in normal subjects was found in the right superior and middle frontal gyri and in the posterior cingulate gyrus (Gardini et al., 2009). The reward dependence dimension has been associated with the thalamo-cingulate subdivision of the limbic system also called the circuit of Papez, “the mechanism of emotion” (Papez, 1937). It is hypothesized to regulate the tonic opposition of social attachment and aloofness by its role in selective attention to salient emotional events (Cloninger and Svrakic, 2000). Persistence is hypothesized to be associated with the ventral striato-thalamic-prefrontal circuit. It seems to regulate reward-guided choice behavior (Schultz et al., 1998). Individual differences in persistence in humans are strongly correlated with responses measured by fMRI in a circuit involving the ventral striatum, orbitofrontal cortex/rostral insula, and prefrontal/cingulate cortex (Gusnard et al., 2001, 2003). In addition, a significant negative correlation between scores on persistence and gray matter volume in normal subjects was found in the right caudate and rectal frontal gyrus (Gardini et al., 2009).

Character is often described as the ability of the human being to act intentionally and purposefully (Self-Directedness); it involves our concepts of self and our relations with other people (Cooperativeness) and the world as a whole (Self-Transcendence). Therefore, character is expression of higher cognitive functions depending on the integrity of the thalamo-neocortical system and centrally integrated in the prefrontal cortex, the principal network in modulating goal-directed behavior

(Nauta, 1971; Fuster, 1997). P300 amplitude in parietal areas is positively correlated with Self-Directedness and Contingent Negative Variation (CNV) amplitude is negatively correlated with Cooperativeness and Self-Transcendence (Cloninger, 1998; Vedeniapin et al., 2001). Furthermore, a recent study showed that the young adult females showed greater Cooperativeness as well as larger relative global and regional gray matter volumes (GMVs) than the matched males, particularly in the social-brain regions including bilateral posterior inferior frontal and left anterior medial prefrontal cortices (Yamasue et al., 2008).

There is a convergent evidence in the literature that both adults and children with ADHD have high level of NS, and low levels of SD and CO. (Donfrancesco et al., 2015; Park et al., 2016; Kim et al., 2017). The same pattern has been found in children with only ODD. Children and adolescents with both ODD and ADHD showed decreased levels of Persistence and Self-directedness (Kim et al., 2010).

From a methodological point of view the subdivision of temperament into four dimensions and character in 3 dimensions (particularly cooperativeness and self-directedness) seemed appropriate to describe the symptomatology of our two groups of patients where some symptoms seem to overlap. While these temperamental and character dimensions are subtended by distributed neural systems, we highlight that a correlation between personality factors and neural networks is necessary to develop methods that study “specific” aspects of the personality. Also, we do not stand only with the results of the clinical scale, but we also pay attention to the neurophysiological findings that distinguish the two groups, which implicitly takes into account the neural systems involved in that differentiation. It is our believe that the combination of both sources of information is what provides the best chance for obtaining a more clear understanding about their differences.

Having said that, the purpose of this study was to identify biomarkers that could distinguish children with ADHD_C from children with ADHD_C + ODD, by combining the results of qEEG and JTCI. It is expected that the combined use of clinical indices together with the EEG spectra at the sources can effectively discriminate the two groups.

2. Methods

2.1. Material

This study was conducted by recruiting consecutive patients from the ADHD Centre of the Child and Adolescent Neuropsychiatry Department of Rho hospital. The following protocol was approved by the Ethical Committee of the hospital.

2.2. Subjects

2.2.1. Inclusion criteria

Fifty Patients between 6 and 15 years of age (28 subjects, 25 males and 3 females, with ADHD_C mean age:10.1, SD:3.1 and 22 subjects with ADHD_C + ODD, 21 males and 1 female, mean age:10.3, SD:2.2) were included in the study if they met all of the following criteria: patients met DSM-V diagnostic criteria for ADHD_C and ADHD_C + ODD, scored at least 1.5 standard deviations above the age norm for their diagnostic subtype using published norms for the Swanson, Nolan, and Pelham–IV Questionnaire (SNAP-IV) (Swanson, 1992) subscale scores, and scored above one of the given cut-offs (T-score > 55) of the Conners subscales based on age and gender (Conners, 1997). Patients scored > 15 points on the narrow band ADHD questionnaires for parents (SDAG) and teachers (SDAI) (Cornoldi et al., 1996). ODD behavior was also evident during clinical examination and during testing. The attitude was provocative and challenging not performing properly the test's instructions, surely not because of lack of understanding or inattention. This oppositional attitude persisted even after the subjects were reprimanded. The response was to continue clearly verbalizing their challenge to authority, claiming that they did not want to change their attitude.

2.2.2. Exclusion criteria

Patients were excluded from the study if they met any of the following criteria: presence of documented psychiatric disorders of the parents, weight < 20 kg at assessment visit, a documented history of Bipolar type I or II disorder, history of psychosis or pervasive developmental disorder, seizure disorder, head injury with loss of consciousness or concussion, migraine, neurological/systemic medical disease (e.g.: lupus, diabetes) or with history of stroke or arteriousvenus malformation or brain surgery. Functional comorbidities such as visual or auditory processing problems were not an exclusion criterion but were documented with IQ testing. Additional exclusion criteria were: serious suicidal risk as assessed by the investigator, history of alcohol or drug abuse within the past 3 months or currently using alcohol or drugs.

2.3. Clinical protocol

The clinical assessment was conducted according to the following protocol. Family history was obtained by clinical interviewing one or both parents. At the first visit, after explaining to the patient and the parent/caretaker the purpose and the procedures of the study, informed consent was obtained from both parents, adolescents and children. Adequate time to consider the information was provided. In the assessment phase the following information was obtained: demographics, medical and psychiatric history, previous and concomitant medications, physical and neurological examination, laboratory samples, Electrocardiogram (ECG), qEEG, Amsterdam Neuropsychological Test (ANT, de Sonneville, 2014) a battery to test executive functions and attention, SNAP-IV ADHD scale revised (SNAP IV – Swanson, 1992; Gaub and Carlson, 1997), Conners' rating scale-R for teachers and parents (CTRS-S-Conners, 1997), narrow band ADHD questionnaires for parents (SDAG) and for teachers (SDAI), Cornoldi et al., 1996). Children Depression Rating Scale, derived from the Hamilton Rating Scale for Depression (HAM-D), Pediatric Anxiety Rating Scale (PARS) were used to exclude mood and anxiety disorders. None of the children had a history of neither pharmacological nor behavioral treatment for their symptoms. Italian version of JTCI of Cloninger (Cloninger et al., 1993) was administered to the parents (Andriola et al., 2012).

The mean IQ (WISC-III) of the subjects with ADHD_C and ADHD_C + ODD was 109,6 SD:12.0, and 102,7 SD:15.8 respectively.

2.3.1. Junior temperament and character inventory (JTCI)

We used the Italian version of JTCI-parent version. It consists of 108 statements to which the parents must answer “true” or “false”. The parent had to report, without time constraint, how his or her child usually acted and felt. The 108 items measure the 7 dimensions of the Cloninger psychobiological model of personality (Cloninger et al., 1993). In the Italian version, (Andriola et al., 2012) also showed that the Parent reports of each of the JTCI dimensions had good internal consistency and test-retest reliability over 3 months.

2.4. Neurophysiologic assessment

2.4.1. EEG data acquisition

Twenty minutes of eyes closed resting EEG were recorded from 19 electrodes, using Electro-caps which place the sensors in accordance with the International 10/20 Electrode Placement System, referenced to linked earlobes. A differential eye channel (diagonally placed above and below the eye orbit) was used for detection of eye movements. All electrode impedances were below 5000 Ω. The EEG amplifiers had a bandpass from 0.5 to 70 Hz (3 dB points). All EEG data were collected on the same digital system compatible with the demands of the protocol in order to achieve amplifier equivalence. A standard calibration system

was provided with the digital EEG machine. Data were sampled at a rate of 256 Hz with 12-bit resolution. To avoid drowsiness during EEG recordings and to guarantee similar conditions throughout the different sessions, all the patients were recorded in the morning, instructed to keep their eyes closed and stay awake. Patients were monitored with a closed-circuit television system, throughout EEG recording. During the recording, the technician was aware of the subject's state to avoid drowsiness.

2.4.2. qEEG at the scalp

The raw EEG data were visually edited by trained EEG technologists, to identify and eliminate biological (e.g., muscle movement, EMG) and non-biological (e.g., electrical noise in the room) artifacts. This was augmented by a computerized artifact detection algorithm. Two minute artifact-free data, collected from the beginning of the EEG recording were then submitted to frequency analysis. The EEG spectra were calculated using the High Resolution Spectral (HRS) model (Pascual-Marqui et al., 1998; Valdes-Sosa et al., 1990; Szava et al., 1993) for all the channels by means of the Fast Fourier Transform (FFT), in a frequency range from 0.39 Hz to 19.11 Hz, with a frequency resolution of 0.39 Hz. The spectra were Log transform, to approach to Gaussianity (John et al., 1980; Gasser et al., 1982) and the *Z*-transform was calculated against the Cuban Normative Database (Szava et al., 1993). Significant test re-test reliability for these measures has been demonstrated (John et al., 1983, 1988; Kondacs and Szabo, 1999).

2.4.3. qEEG source analysis (qEEGT)

2.4.3.1. Source density localization. The source density localization analysis was performed for frequencies between 0.39 and 20 Hz and for all the sources in the cerebral cortex for a grid of 3244 sources. The Variable Resolution Electrical Tomography (VARETA) method (Bosch-Bayard et al., 2001) was used in the source localization analysis. VARETA is a technique for estimating the distribution of the primary current in the source generators of EEG data. Like LORETA (Pascual-Marqui et al., 1998), VARETA is a Discrete Spline Distributed Solution. Spline estimates are the spatially-smoothest solutions compatible with the observed data. VARETA applies different amounts of spatial smoothing for different types of generators, with the actual degree of smoothness in each voxel being determined by the data itself; hence the use of the term variable resolution. VARETA allows spatially-adaptive nonlinear estimates of current sources and eliminates the “ghost solutions” (artifactual interference patterns) often present in linearly-distributed inverse solutions. In this way, VARETA produces focal solutions for point sources, as well as distributed solutions for diffuse sources. In addition, anatomical constraints are placed upon the allowable solutions by introducing a “gray matter weight” for each voxel. The effect of these weights on the inverse solution is to prohibit sources in which the mask is zero (for example, CSF or white matter). A three-concentric spheres Lead Field (Riera and Fuentes, 1998), defined over a grid of 3244 points located in the gray matter of the Montreal Neurological Institute (MNI) template (Evans et al., 1993, 1994) was used to solve the forward EEG problem and generating the voltage at the 19 electrodes of the 10–20 System.

The EEG activity was re-referenced to the average reference at each time point for this analysis, as required by VARETA and other inverse solution methods. To render the inverse solution in different subjects comparable for statistics at the sources, VARETA uses the same regularization parameter for all subjects. The value for this parameter is obtained from the subjects in the normative database, and it was also used for the norms calculations. After transformation to the average reference, the geometric power is applied to standardize by a global scale factor to control for individual differences in power values due to skull thickness, hair volume, electrode impedance, and other factors of variance that can affect EEG amplitudes but are not related to electrophysiological variability. This procedure is described in detail elsewhere (Bosch-Bayard et al., 2001). The anatomical accuracy of the functional qEEG source localization obtained by VARETA and other methods has been repeatedly confirmed by co-registration with other brain imaging modalities e.g. functional magnetic resonance, fMRI (Mulert et al., 2004), positron emission tomography, PET (Zumsteg et al., 2005; Bolwig et al., 2007), and computerized tomography (Prichep et al., 2001). It has also been used satisfactorily for source localization in psychiatric patients with insomnia (Corsi-Cabrera et al., 2012).

Two minutes of artifact-free EEG were also submitted for the computation of the spectra at the EEG sources using Variable Resolution Electrical Tomography (VARETA) (Bosch-Bayard et al., 2001). The EEG sources were located using a grid defined over the gray matter of the probabilistic MRI Brain Atlas (Evans et al., 1993). The standard positions of the International 1020 electrodes positioning system were used for the Lead Field calculation (Riera and Fuentes, 1998). With this Lead Field, VARETA was applied to the cross-spectral matrices calculated for all frequencies and leads at the scalp, to calculate the spectra at the sources space with the same frequency resolution (from 0.39 to 20 Hz with a frequency resolution of 0.39 Hz: high spectral resolution, HSR). Obtaining the value of the spectra for every source of the gray matter at each frequency constitutes a new type of Neuroimaging technique that has been termed Quantitative EEG Tomographic Analysis (qEEGT) (Bosch-Bayard et al., 2001).

To account for age differences, the *Z*-spectra were computed relative to the normative values of the Cuban Normative Database. The sources were then superimposed upon MRI slices of the MNI Atlas (Evans et al., 1993), and the values computed for each frequency in every voxel were encoded using a color palette with hues proportional to the standard- or *Z*-scores of deviations from expected normative values. The significance levels of the images are corrected for the large number of comparisons by using the random fields theory, introduced by Worsley et al. (1995). This approach proposes a unified statistical theory for assessing the significance of apparent signal observed in noisy difference images, giving an estimate of the corrected *p*-value for local maxima of Gaussian fields over search regions of any shape or size in any number of dimensions.

2.5. Statistical analyses

As a first step, to assess whether there were statistical differences of the scores of the JTCI between the two groups, a MANCOVA test was performed: the group was included as a categorical factor and the IQ and Age were included as two continuous factors. They were tested against the dependent vector conformed by 7 dimensions of TCI. The only significant effect was the Group effect. Neither the Age or IQ were significant.

To further validate this result, an additional ANCOVA test was performed, using a univariate model for each variable. This analysis revealed that there were significant differences only for the variables NS and SD between the groups. The results are summarized in Table 1. These results were also validated by an additional univariate *t*-test for the JTCI variables, which also showed significant effects only for NS and SD.

A more detailed discussion of these results is given in Section 3.1.

2.5.1. Stability based biomarkers identification methodology

The methodology used in this paper has been described in detail in Bosch-Bayard et al., 2018. In summary, to achieve stability and robustness, the method is divided in two steps, based on subsampling both for the parameter estimation as well as for the validation procedure. In the first step, a random subsample of the original sample is generated using the 30% of the variables and the 70% of the subjects. A classification procedure is applied to this subsample. In our case we use the General Linear Model via elastic net (GLMNet, Friedman et al., 2008) which is a logistic penalized regression method. This method extracts a sparse subset of classifiers from the whole set of variables,

Table 1
ANCOVA results for the univariate model of all JTCI variables.

	DF	NS		HA		RD		PS		SD		CO		ST	
		F	p	F	p	F	p	F	p	F	P	F	p	F	p
Intercept	1	1,06	0,31	5,46	0,024	0,44	0,51	0,84	0,37	1,86	0,18	2,76	0,10	0,80	0,38
Age	1	0,14	0,71	3,65	0,06	0,31	0,58	0,02	0,9	0,17	0,69	0,05	0,82	0,02	0,89
IQ	1	0,09	0,76	2,75	0,10	0,57	0,46	0,03	0,87	0,25	0,62	3,89	0,055	1,13	0,29
Group	1	12,15	0,001	2,52	0,12	0,91	0,35	0,46	0,50	14,57	0,0004	0,91	0,35	1,74	0,20
Total	48														

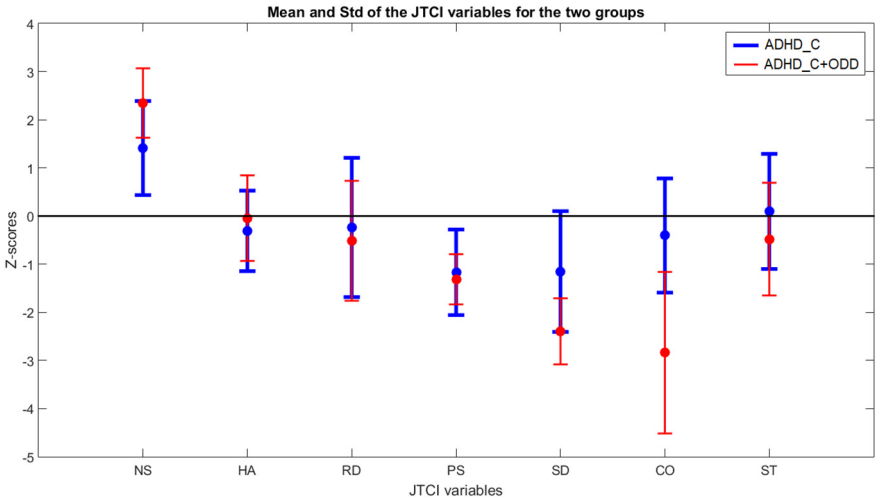

Fig. 1. Z-scores and SD of the variables of the JTCI scale for the two groups. NS = novelty seeking, HA = harm avoidance, RD = reward dependence, P = persistence, SD = self-directedness, CO = cooperativeness, ST = self-transcendence.

while discarding the rest. The random procedure is repeated a sufficiently number of times (500 times in our case). In each realization, the classifiers are kept. Those variables which were selected as classifiers in at least 50% of the times participated in the classification procedure and stored as the more stable biomarkers. With these variables, the final classification equation is built. The ROC technique is used to measure the classification power of the selected set of biomarkers. To ensure a more stable estimation of the area under the curve, again the subsampling technique is used. In this case, all biomarkers are kept while generating a subsample with about the 70% of the subjects. The ROC area is calculated for the 10, 20 and 100% of False Positive (FP) and these numbers are stored. The procedure is randomly repeated a sufficiently high number of times (500 in our case). With these values, empirical distributions of the ROC values are obtained at the three levels of FP. The values of these distributions at the 50% of the curve are given as the stable estimate of area under the ROC, which characterizes the predictive classification power of the selected set of biomarkers.

2.5.2. Biomarkers identification at the source level

As second step, instead of staying at scalp level, we also applied the technique to the source spectra obtained with the qEEGT procedure. Both approaches have their intrinsic value and serve for different purposes: obtaining the best set of classifiers at the scalp level, if successful, would allow us, for example, to design specific purpose EEG recording devices with the smallest number of electrodes, able to identify clinical subgroups. This may be useful in epidemiologic studies in which it is necessary to identify persons at risk in big populations. On the second hand, applying the procedure at the source level, would allow us to identify the brain regions more directly related to the distinction between subgroups, which is our final goal from the research point of view. From the methodological point of view, while the procedure at the scalp give less information about the brain areas, the number of variables participating in the selection procedure is smaller, which allows for a better performing of the selection methodology because the number of random repetitions may cover more combinations of the original space.

To clarify the previous sentence, in our study, when applying the GLMNet method for the Biomarkers identification at the source level, the number of variables is extremely high (3623 sources × 49 frequencies = 159,887 variables). One strategy is to use the Brain Atlas Segmentation (67 regions) where voxels activity in an area is averaged. This method has advantages like: 1) statistically more robust (diminishes the effect of outliers) and 2) increases the chances of regions to become biomarkers because of a smaller number of variables. But, on the other hand, if the region is big and few voxels are significant, the average can mask those significant voxels activity. Furthermore, the problem size still exists after Atlasing: 67 regions × 49 freqs = 3283 variables. In order to reduce the number of variables we decided to apply the preprocessing step proposed in Bosch-Bayard et al. (2018) named “indfeat” (Weiss and Indurkhya, 1998). It consists in performing univariate *t*-tests for each variable between the two groups and eliminating those variables which indfeat indices lower to 1. In this way we reduced the number of variables to 604. The 7 TCI measurements were also included in the analysis.

3. Results

3.1. Behavioral results

Fig. 1 shows the mean and SD for the *Z*-score of the variables of the JTCI scale for the two groups. The temperament of children with ADHD_C and ADHD_C + ODD showed differences when compared to norms. Both groups exhibited higher values of novelty seeking and lower values of self-directedness and cooperativeness. However,

subjects with ADHD_C + ODDs had even significantly higher levels of novelty seeking and lower level of Self-Directedness and Cooperativeness than subjects with ADHD_C.

A MANCOVA analysis of the scores of the JTCI Temperament scale between the two groups, with the group as a categorical factor and two continuous factors (IQ and Age), showed that the only significant effect was the Group ($F = 3.52$; df = [7,39]; $p < 0.01$). Neither the Age nor IQ were significant (age: $F = 0.51$; df = [7,39]; $p > 0.8$; IQ: $F = 1.06$; df = [7,39]; $p > 0.4$). For this model, we didn't find significant differences between the slopes of the two groups. An additional ANCOVA test, using a univariate model for each variable of the JTCI, revealed that there were significant differences between the groups only for the variables Novelty Seeking and Self-directedness. The ADHD_C + ODD had in the temperament domain higher z score values of novelty seeking than the ADHD_C children and in the character, domain had lower Z score value of self-directedness compared with children with ADHD_C (Table 1). Since no significant effects were found in the independent variables, the *t*-test was also used. The univariate t-test of each variable, showed significant results between the groups only for NS ($t = -3.46$; df = 46; $p < 0.001$); SD ($t = 4.52$; df = 46; $p < 0.0001$) and CO ($t = 5.83$; df = 46; $p < 0.0001$).

3.2. Biomarkers results

We applied the biomarkers selection methodology to the *Z*-scores of the JTCI scale as well as to the Z-spectra at the electrodes and at the sources separately. Then we applied the same methodology to the Z-spectra at the electrodes combined with the JTCI Z-scores (Z-spectra + Z-JTCI) and to the Z-spectra at the sources combined with the JTCI *Z*-scores (Z-sources + Z-JTCI). The discrimination power of each classification equation was measured by the robust area under the ROC (rAUC) at the 10%, 20% and the total area. The results are summarized in Table 2.

As it can be observed in Table 2, the best discrimination power was obtained when the JTCI Z-scores were combined with the qEEG or the qEEGT parameters. This was especially evident at a low rate of False Positives (10% and 20%) which is a very desirable characteristic in a classifier, since a high number of True Positive are identified at a cost of a low number of False Positive.

The procedure was also carried out with the Log of the raw values of the spectra both at the electrodes (qEEG parameters) and at the sources (qEEGT parameters). In both cases, the discrimination power of the classification equations was higher with the *Z*-values than with the log of the raw values. Therefore, in what follows, we will report the results obtained using the *Z*-values of the qEEG and the qEEGT parameters, combined with Z-scores of the JTCI scale.

The procedure was also applied to the Absolute Power of the traditional Broad Band model (Delta: 1.5–3.5 Hz; Theta 3.9–7.2 Hz; Alpha: 7.5–12.5 Hz and Beta: 12.8–19.11 Hz), again separately and combined with the Z-scores of the JTCI scale. The discrimination power obtained with these datasets was significantly worse than the ones obtained with the HRS model. Our conclusion regarding these results is that summarizing by frequencies is not a good choice for the classification purpose, since averaging among frequencies may mask or cancel out the differences between groups present in specific frequencies.

Table 2
Robust AUC values (rAUC) at the 10% and 20% of false positives as well as the total AUC obtained by the biomarkers identification methodology, applied to each set of variables separately and combined.

Dataset	# of variables	rAUC (10%)	rAUC (20%)	rAUC (Total)
Z-JTCI	7	0.59	0.70	0.88
Z-spectra	912	0.48	0.66	0.80
Z-sources	3283	0.61	0.72	0.81
Z-JTCI + Z-spectra	919	0.89	0.95	0.95
Z-JTCI + Z-sources	3290	0.78	0.86	0.91

Table 3
Best set of classifiers obtained for the Z-scores of JTCI scale combined with the Z-values of the qEEG parameters (scalp).

Variable	Origin	Frequency	Frequency band	φ coefficients
Novelty seeking	JTCI			0.0255
Self-directedness	JTCI			−0.0912
Cooperativeness	JTCI			−0.0985
F4	EEG	1.17 Hz	DELTA	−0.0593
F4	EEG	1.56 Hz		−0.2581
Cz	EEG	1.56 Hz		−0.1768
Fz	EEG	4.30 Hz	THETA	0.3155
F4	EEG	5.47 Hz		0.1129
F7	EEG	15.62 Hz	BETA	−0.1284
F8	EEG	17.58 Hz		−0.0589

Table 4
Best set of classifiers obtained for the Z-scores of JTCI scale combined with the Z-values of the qEEGT parameters (sources).

Variable	Origin	Frequency	Frequency band	φ coefficients
Novelty seeking	JTCI			0.0334
Self-directedness	JTCI			−0.0644
Cooperativeness	JTCI			−0.0957
Insula left	EEG	4.68 Hz	THETA	0.1057
Lat. orbito-frontal gyrus right	EEG	6.63 Hz		−0.1037
Lat. orbito-frontal gyrus right	EEG	8.97 Hz	ALPHA	0.0692
Lat. orbito-frontal gyrus right	EEG	9.36 Hz		0.0300
Cingular region right	EEG	9.36 Hz		0.0182
Lat. orbito-frontal gyrus right	EEG	9.75 Hz		0.0153
Lat. orbito-frontal gyrus right	EEG	11.31 Hz		−0.0835
Angular gyrus right	EEG	11.7 Hz		0.1284
Inf. occipital gyrus right	EEG	17.55 Hz	BETA	−0.0849
Occipital pole left	EEG	17.55 Hz		−0.0093
Lat. orbito-frontal gyrus right	EEG	19.11 Hz		−0.0460
Medial orbitofrontal gyrus right	EEG	19.11 Hz		−0.0506

Tables 3 and 4 show the classification equations obtained by the biomarkers selection methodology for the data sets composed by the combinations of the *Z*-scores of the JTCI scale with the Z-spectra at the electrodes (qEEG) and the Z-spectra at the sources (qEEGT) respectively. In both, the first three variables participating in the equation belong to the JTCI scale and the rest to the qEEG/qEEGT parameters. In each table, it is specified the name of the electrode (qEEG) or the brain region (qEEGT) selected as well as the frequency in which they were selected as biomarkers. The last column of each table (φ Coefficients) shows the coefficient that accompanies each variable in the classification equation.

In both cases, Self-directedness (SD) and Cooperativeness (CO) of the JTCI scale were selected in > 90% of the times, Novelty Seeking (NS) was selected about 70% of the times. SD, CO and NS participated in the classification procedure.

Fig. 2 shows the topographical distribution of the biomarkers selected from the qEEG parameters, summarized by frequency bands. In Delta band, F4 and Cz, in Theta band Fz and F4 electrodes, in Beta band F7 and F8 were selected.

Fig. 3 shows the brain regions selected as biomarkers from the qEEGT parameters at the sources level. In Theta band the left insula and the right lateral fronto- orbital gyrus were selected. In Alpha band the most significant regions were the right lateral fronto-orbital gyrus, the right angular gyrus, and the right cingular region. In Beta band, the

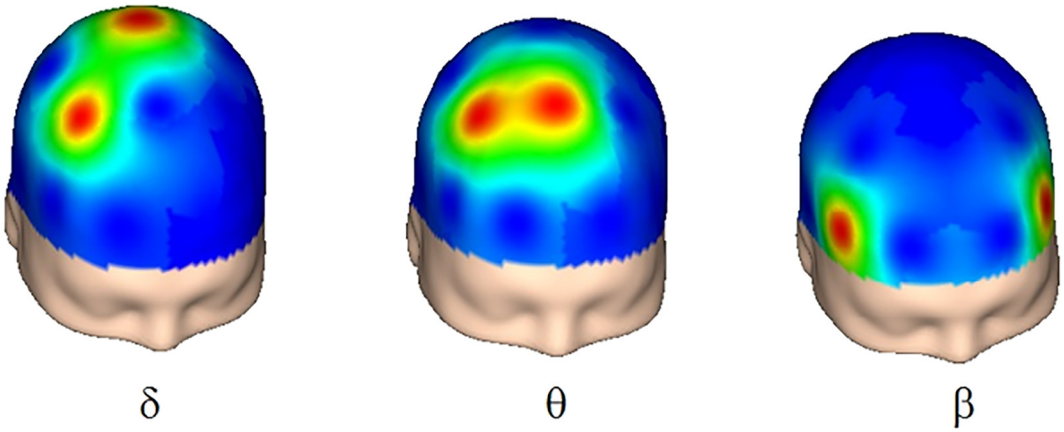

Fig. 2. Topographical distribution of the biomarkers in the different traditional Broad Band Models. In Delta band, only F4 and Cz; in Theta band only Fz and F4; in Beta band F7 and F8 were selected.

most significant sources were the right lateral fronto-orbital gyrus, the right medial fronto-orbital gyrus, the right inferior occipital gyrus and the left occipital pole. The orbito-frontal cortex (OFC), therefore, is the area most present in all frequency bands except delta band where no regions of interest were present (see also Table 4).

The classification power of the two equations (at the scalp and at the sources) is shown in Fig. 4. The left side of the figure shows the results obtained by the biomarkers at the scalp and the right side shows the results of the obtained by the biomarkers at the sources. The upper part contains boxplots which show the mean, standard deviation and quantiles for the two groups for both equations. The scatterplots inside the boxplots show the score of each subject in each group for the two classification equations, at the scalp and at the sources respectively. The lower part of the figure shows the two robust ROC curves estimated by the stability procedure.

As an additional step, to understand how the variables selected as biomarkers behaved in each group, we calculated linear regression equations for each variable using the Group as the independent variable. In this way, the sign of the slope (m) of the linear equation indicates which of the groups had bigger values for the variable. Since ADHD_C was before ADHD_C + ODD, a positive sign of m indicates that ADHD_C had lower values than ADHD_C + ODD and vice versa. Table 5 shows the values and the significance (p) of the slope of the Z-scores of the JTCI scale selected as biomarkers; Table 6 shows the values and the significance (p) of the slope of the biomarkers selected from the qEEG parameters at the scalp and Table 7 shows the values and the significance (p) of the slope of the biomarkers selected from the qEEGT parameters at the sources. Note that NS, SD and CO showed a highly significant slope between the groups. However, from the qEEG and qEEGT parameters, only in the right hemisphere there were the most significant differences: F4 at 1.7 Hz, F4 at 5.4 Hz and F8 at 17.5 Hz had significant regression values, while the rest of the variables considered

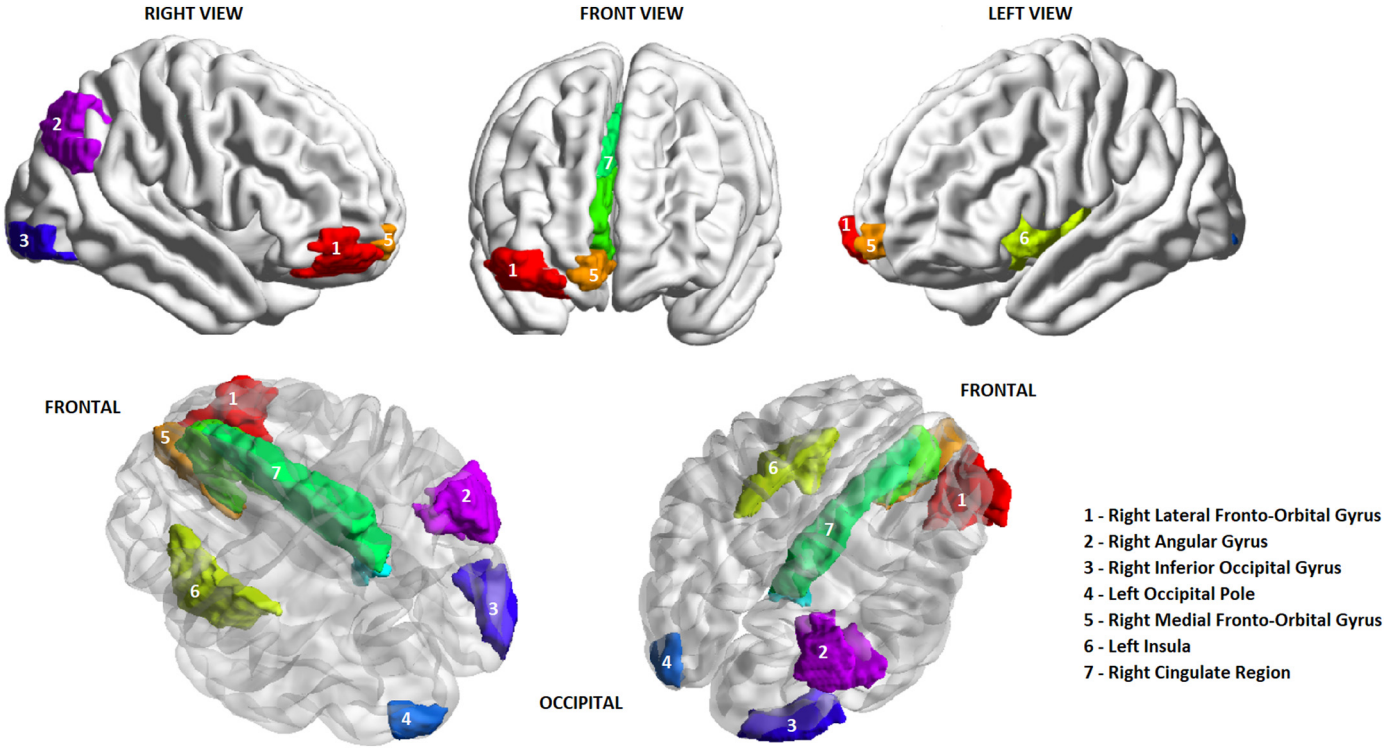

Fig. 3. Tomographical distribution of the biomarkers at the sources, showing the brain regions selected as biomarkers: Left Insula, Right lat. Orbito-frontal gyrus right, right Cingular region, Right Angular gyrus, Right Inf. Occipital gyrus, Left Occipital pole, Right medial Orbito-frontal gyrus.

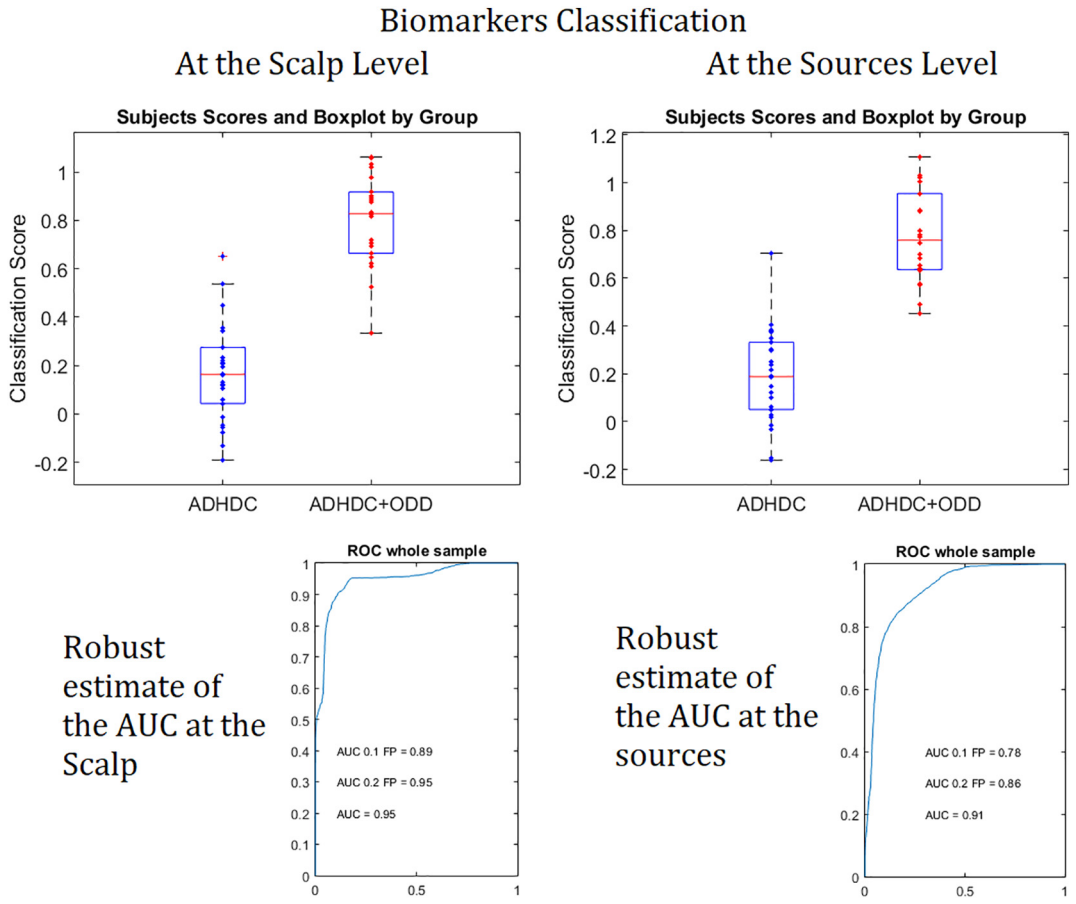

Fig. 4. Classification power of the two equations at the scalp level (left side) and at the sources (right side). The upper part contains boxplots which show the mean, standard deviation and quantiles for the two groups for both equations. The scatterplots inside the boxplots show the score of each subject in each group for the two classification equations, at the scalp and at the sources respectively. The lower part of the figure shows the two robust ROC curves estimated by the stability procedure.

Table 5
Slope value (m) and Significance (p) of the linear regression between the two groups for the biomarkers selected from the JTCI scale.

Variable	m(slope)	p
Novelty seeking	0.86	0.0015
Self-directedness	−1.3	9.2e-6
Cooperativeness	−2.4	2.3e-6

Table 6
Slope value (m) and Significance (p) of the linear regression between the two groups for the biomarkers selected from the qEEG parameters (scalp).

Variable	Frequency	Frequency band	m(slope)	p
F4	1.17 Hz	DELTA	−0.24	0.05
F4	1.56 Hz		−0.19	0.08
Cz	1.56 Hz		−0.06	0.6
Fz	4.30 Hz	THETA	−0.14	0.19
F4	5.47 Hz		−0.21	0.03
F7	15.62 Hz	BETA	0.03	0.74
F8	17.58 Hz		−0.21	0.004

separately didn't show a significant regression between groups. The children with ADHD_C had significantly greater activity in those frequency bands than the ADHD_C + ODD.

Table 7
Slope values (m) and Significance (p) of the linear regression between the two groups for the biomarkers selected from the qEEGT parameters (sources).

Variable	Frequency	Frequency Band	t-Values	p
Insula left	4.68 Hz	THETA	0.25	0.16
Lat. orbito-frontal gyrus right	6.63 Hz		−0.041	0.84
Lat. orbito-frontal gyrus right	8.97 Hz	ALPHA	0.028	0.88
Lat. orbito-frontal gyrus right	9.36 Hz		0.0014	0.99
Cingular region right	9.36 Hz		0.022	0.92
Lat. orbito-frontal gyrus right	9.75 Hz		0.19	0.23
Lat. orbito-frontal gyrus right	11.31 Hz		0.052	0.72
Angular gyrus right	11.7 Hz		0.14	0.43
Inf. occipital gyrus right	17.55 Hz	BETA	−0.3	0.22
Occipital pole left	17.55 Hz		−0.32	0.17
Lat. orbito-frontal gyrus right	19.11 Hz		−0.122	0.58
Medial Orbitofrontal gyrus right	19.11 Hz		−0.11	0.66

4. Discussion

Bosch-Bayard et al. (2018) have given strong evidence of the validity and robustness of the biomarkers selection procedure based on the GLMNet method. GLMNet itself has also been successfully applied in different clinical situations (Casanova et al., 2011; Hernandez-Gonzales et al., 2011). The fact that, to our knowledge, this method of combining behavioral and neurophysiological data in the same classification procedure has been applied for the first time is of particular relevance in this context since we were able to obtain the best classifiers that discriminated the two groups.

The best results were obtained when the methodology was applied by combining JTCI values (behavioral level) and the z values (instead of raw spectra scores) of the qEEG (scalp) or qEEGT (sources) parameters (neurophysiological level). In both procedures (at the scalp and at the sources level), the JTCI measurements of NS, SD and CO were selected as biomarkers. At the scalp level, the best classifiers from the qEEG parameters were F4 and Cz in the delta band; F4 and Fz in theta band and F7 and F8 in beta band (15.6 and 17.5 Hz respectively) (see Table 3). The discrimination power of the classification equation obtained with this data, validated by the robust ROC estimation (Bosch-Bayard et al., 2018), was of 0.95 for the Total AUC, 0.89 at a 10% of FP and 0.95 at a 20% of FP. The left upper panel of Fig. 4 shows a boxplot with the discrimination between the two groups obtained by this procedure. It can be noted that there is an almost perfect separation between the groups, which explains the high value obtained for the robust area under the ROC. The scatterplot inside the boxplot shows the score of each subject. The lower left panel of the figure shows the stable ROC curve estimation obtained by the stability procedure.

At the sources level, the selected biomarkers were the left insula and the right lateral fronto-orbital gyrus in Theta band; the right lateral fronto-orbital gyrus, the right angular gyrus, and the right Cingular region in Alpha band; and the right lateral fronto-orbital gyrus, the right medial fronto-orbital gyrus, the right inferior occipital gyrus and the left occipital pole in Beta band. The orbito-frontal cortex (OFC), therefore, is the area most present in all frequency bands except delta band where no biomarkers were selected (see Table 4). The robust estimation of the AUC for this classification equation was of 0.91 for the Total area, 0.78 at a 10% of FP and 0.86 at a 20% of FP. The right upper panel of Fig. 4 shows a boxplot of the discrimination between the two groups at the sources. The scatterplot inside the boxplot show the score of each subject. Compared to the scalp, the classification at the sources is even better than at the scalp: the groups are more compact and separated. The lowest values of the AUC, especially at the 10% and 20% rate of False positives are explained for the existence of an outlier in the ADHDC groups, who is mixing the distributions. The lower left panel of the figure shows the stable ROC curve estimation obtained by the stability procedure at the sources.

Although the results at the sources level showed a high classification power of the equation, they may be influenced by the approaches used in this work, especially the summarization by brain regions. The number of variables to be considered at the source level is extremely high. In this work we used a summarization by brain regions. However, in Fig. 3 it can be noted that some of the selected areas are rather big. Moreover, some of the not selected areas are even bigger. One brain region may be related to different functions. If the area that is responding to a specific function is only a small part of a large region, then when summarizing the whole area, the function of this small part may not be well represented in the whole average of the region. This may cause that the specific area does not appear as biomarker. To solve this problem, some procedures still should be tested: a) using a finer brain segmentation, which produces small areas; b) using a priori knowledge to restrict the number of sources (or areas) to be included in the analysis; c) applying some a priori statistical test to eliminate sources/areas which do not contain information to differentiate the groups (for example where there are not significant differences between the groups); or d) performing a priori algorithms, like principal components analysis, to select the areas to be considered in a data driven procedure. These alternatives should be considered in the future to improve the performance of the classification equation.

From a visual inspection of Tables 6 and 7 it can be noted that, when analyzed separately, the majority of the variables that were selected as biomarkers, do not have high classification power to differentiate the groups: only the three JTCI variables (NS, SD and CO), F4 at 1.1 and 5.4 Hz and F8 at 17.5 Hz reached a significant regression between the groups (p value of the slope regression). However, the classification equation has a high classification power. Therefore, it is not each variable by itself but the combination of all of them (the behavioral as well as the neurophysiological ones) that produced the equation with the high classification power. This is one of the strengths of the used method.

Another strength of this method is that, by construction, the obtained results should not be attributed to overfitting, as it has been demonstrated in Bosch-Bayard et al. (2018). In this way, the method guarantees the extraction of a classification equation, with a small number of biomarkers and a stable statistical behavior, i.e., the obtained equation has a high statistical power and is not very sensible to small perturbations in the data.

4.1. Results at the behavioral level

The temperament of children with ADHD_C and ADHD_C + ODD showed higher values of novelty seeking compared to norms. Also, in the character domain, both groups exhibited lower values of self-directedness and cooperativeness compared to norms. However, when the two groups were compared to each other, subjects with ADHD_C + ODDs had significantly higher level of novelty seeking and lower level of Self-Directedness and Cooperativeness than subjects with ADHD_C. These results are compatible with Barkley's (1997a, 1997b, 1997c, 2006) model that interprets these behavioral disorders as a problem of regulation of inhibitory control at all levels: affective, emotional, motivational and linguistic. Children with high values of novelty seeking are children who have the tendency to react to new stimuli or signals of approval or potential punishments. It implies that they need elevated levels of stimulation, and they have the tendency of exploration and enthusiasm, but they are impulsive and ease to get bored. They are messy, fickle, excitable, irritable, and unstable in personal relationships and have sudden bursts of anger. The temperamental dimension of NS, is more pronounced in subjects with ADHD_C + ODD than ADHD_C. The clinical symptomatology reported by the parents and teachers together with the clinical observations fully confirms these results. Melegari et al. (2015) reported that the ADHD children showed a temperamental profile characterized by high Novelty Seeking, low Reward Dependence and low Persistence. Meanwhile, the ODD children shared the high Novelty Seeking with the ADHD children, but they showed higher Persistence than the ADHD children.

Although in our sample we didn't find significant differences in persistence between the two groups, probably because they had in common the ADHD_C, both groups were less persistent compared to norms. Children with low persistence values appear unable to maintain consistent behavior in front of intermittent reinforcements. Low values of persistence reflect lack of perseverance, determination and consistency; therefore, in front of frustration and fatigue these children are inclined to abandon the tasks. These features appear to be one of the clinical characteristic of ADHD.

As the character is concerned, subjects with ADHD_C + ODD showed a significant lower capacity of Self-Directedness (SD) and Cooperativeness (CO) compared to the subjects with ADHD_C. Children with low SD appear aimless, inept, just unproductive and easily blaming others. Low SD stands for immaturity, childishness, lack of self-sufficiency, responsibility and reliability. They are not responsible for their own actions and have low self-esteem and self-confidence. Children with low CO are prejudiced, insensitive, hostile, revengeful, opportunistic and disloyal. All these characteristics are more pronounced in ADHD_C + ODD children.

4.2. Biomarkers results

Significant differences between the groups were found in the absolute power spectra z-score in the right hemisphere (F4 at 1.7 Hz and at 5.4 Hz and F8 at 17.5 Hz) The group of children with ADHD_C had significant higher values in the delta, theta and beta bands than e group of children with ADHD_C + ODD. It has been frequently reported that

children with ADHD have EEG patterns consisting of elevated delta and theta absolute power with deficit or excess of beta activity. This profile has been found primarily in children with the combined type of ADHD (Chabot et al., 1999; Clarke et al., 2001). F4 and F8 cover part of the prefrontal cortex and middle frontal gyrus and in particular the dorsolateral prefrontal cortex. These areas play a fundamental role in several executive functions, executive control of behavior" (Kübler et al., 2006), inferential reasoning (Goel et al., 1997; Knauff et al., 2002), decision making (Rogers et al., 1999). These functions are impaired in children with ADHD_C (Barkley, 1997a, 1997b; Barkley et al., 1992; Goodyear and Hynd, 1992). These two groups of children that have in common ADHD_C seem to lack in the executive control of behavior. It is also known that these areas of the right hemisphere are involved in modulating emotions, reacting properly to stressful situations, understanding other intentions for deciding appropriate behavior. Children with ADHD_C + ODD appear more dysregulated in modulating social behavior and in the control of mood and motivational drive, function(s) that are important components of the personality of an individual.

The biomarkers at the sources identification level confirmed the above results at the electrode sites and showed the regions that best classified the 2 groups.

Many researches support that the main disorders associated with dysregulated OFC connectivity/circuitry are related with decision-making, emotion regulation, and reward expectation (Paulus et al., 2002; Toplak et al., 2005; Verdejo-Garcia et al., 2006). More specifically, a large meta-analysis of the existing neuroimaging studies demonstrated that activity in medial parts of the OFC is related to the monitoring, learning, and memory of the reward value of reinforcers, whereas activity in lateral OFC is related to the evaluation of punishers, which may lead to a change in ongoing behavior (Ernst et al., 2004; Kringelbach, 2005; Kringelbach and Rolls, 2004). OFC seems to be important in signaling the expected rewards/punishments of an action given the details of a situation. In doing this, the brain can compare the expected reward/punishment with the actual delivery of reward/punishment, thus making the OFC critical for adaptive learning (Schoenbaum et al., 2011). Significant positive correlations were observed between scores of novelty seeking and cerebral blood flow in the orbital prefrontal network, particularly the anterior cingulate, the right anterior and posterior insula (Sugiura et al., 2000). It has been reported that children with ADHD showed a decrease in total cerebral volume and total cortical volume reduction throughout the cortex. The ADHD group also showed a significant decrease in cortical folding in all four lobes bilaterally. After correction for multiple comparisons, this effect was only observed in the right frontal lobe (Wolosin et al., 2009). These recent findings add evidence to the notion of dysfunction of this neural circuitry controlling motivation, reward, and impulsivity, including the OFC.

Self-directedness significantly correlates with changes in the medial prefrontal network (Brodmann areas 8/9, BA8/9), suggesting deficit of executive functions as lack of initiative, inability to organize or prioritize activities (Damasio, 1985; Joseph, 1999). Self-directedness was strongly correlated with fMRI response magnitudes in BA9/10 when subjects were carrying out simple executive tasks (Gusnard et al., 2001). Self-directedness was also negatively correlated with reaction times of the same task. Likewise, Bechara et al. (1994, 1996, 1997, 1998) have found that patients with bilateral medial prefrontal lesions cannot anticipate future positive or negative consequences of their actions. It has been also reported that self-directedness in individuals with either borderline or antisocial personality disorder is associated with low activity in the medial prefrontal network) and low cooperativeness with low activity in the orbital prefrontal network. (London et al., 2000; Soloff et al., 2000). Yamasue et al. (2008) have identified for the first time the areas of the brain strongly correlated with cooperativeness: the bilateral posterior inferior frontal gyrus and the antero medial prefrontal cortices. The sources localization method has shown that these areas are dysregulated, and the TCI confirmed this evidence showing that the children with ADHD_C + ODD have less human altruistic cooperation than children with ADHD_C.

The cingulate cortex is an integral part of the limbic system, which is involved with emotion formation and processing, learning, and memory (Lane et al., 1998). Neuroimaging studies show that separate areas of anterior cingulate cortex are involved in cognition and emotion and therefore it can be proposed as an interface that integrates the traits of temperament with those of character (Cloninger, 2002). Bush et al. (1999) have reported that subjects with ADHD failed to activate the anterior cingulate cortex (ACC) during a counting Stroop test and activated the fronto-striatal-insular network, indicating ACC hypo-activity of this region.

The insula together with the anterior cingulate cortex are considered the critical areas of the "salience network," believed to be involved in consciousness. It regulates diverse functions linked to emotion or the regulation of the body's homeostasis. Young patients with ADHD were found to have a bilateral reduction in anterior insular cortex (AIC) gray matter volumes compared to healthy controls. Furthermore, the left AIC was found to positively correlate with oppositional symptoms, while the right AIC was found to associate with both attention problems and inhibition (Lopez-Larson et al., 2012).

The angular gyrus is part of the Default Mode Network (DMN). The DMN function assists in processing and understanding a person's internal, reflective world and the world of self and others. Russell-Chapin et al. (2013) have reported that children with ADHD have difficulty activating the DMN in a resting or quiet state.

In conclusion, the correlation between temperament, character and cerebral function are weak or inconsistent, unless it doesn't pay attention to a specific temperament or a specific cerebral region with its connections. This is the case when TCI dimensions are analyzed together with qEEG data with source level analysis. These methods open the way for a new and original approach to associate differences of personality and behavior to specific neuronal systems and subsystems and could provide a powerful tool for understanding pathophysiology of behavioral disorders.

Funding statement

This research has been partially supported by Grant PAPIIT IA201417, DGAPA-UNAM, Mexico.

References

American Psychiatric Association, 2013. Diagnostic and Statistical Manual of Mental Disorders, Fifth Edition. American Psychiatric Association, Arlington, VA.
Andriola, E., Donfrancesco, R., Zaninotto, S., Di Trani, M., Cruciani, A.C., Innocenzi, M., Maranoi, A., Pommella, L., Cloninger, R.C., 2012. The junior temperament character inventory (JTCI): Italian validation of a questionnaire for the measurement of personality from ages 6 to 16 years. Compr. Psychiatry 16.
Barkley, R., 1997a. ADHD and the Nature of Self-Control. The Guilford Press, New York (410pp).
Barkley, R., 1997b. Attention-deficit/hyperactivity disorder, self-regulation and time: toward a more comprehensive theory. Dev. Beh. Paediatr. 18, 271–279.
Barkley, R.A., 1997c. Behavioral inhibition, sustained attention, and executive functions: constructing a unifying theory of ADHD. Psychol. Bull. 121, 65–94.
Barkley, R., 2006. Attention-deficit/hyperactivity disorder. In: A Handbook for Diagnosis and Treatment. The Guilford Press, New York, pp. 770.
Barkley, R.A., Grodzinsky, G., DuPaul, G., 1992. Frontal lobe functions in attention deficit disorder with and without hyperactivity: a review and research report. J. Abnorm. Child Psychol. 20, 163–188.
Barry, R.J., Clarke, A.R., 2009. Spontaneous EEG oscillations in children, adolescents, and adults Typical development, and pathological aspects in relation to AD/HD. J. Psychophysiol. 23 (4), 157–173.
Barry, R.J., Clarke, A.R., Johnstone, S.J., 2003. A review of electrophysiology in attention-deficit/hyperactivity disorder: I. Qualitative and quantitative electroencephalography. Clin. Neurophysiol. 114, 171–183.
Bechara, A., Damasio, A.R., Damasio, H., Anderson, S.W., 1994. Insensitivity to future consequences following damage to human prefrontal cortex. Cognition 50, 7–15.
Bechara, A., Tranel, D., Damasio, H., Damasio, A.R., 1996. Failure to respond autonomically to anticipated future outcomes following damage to prefrontal cortex. Cereb. Cortex 6, 215–225.
Bechara, A., Damasio, H., Tranel, D., Damasio, A.R., 1997. Deciding advantageously

before knowing the advantageous strategy. Science 275, 1293–1295.
Bechara, A., Damasio, H., Tranel, D., Anderson, S.W., 1998. Dissociation of working memory from decision making within the human prefrontal cortex. J. Neurosci. 18, 428–437.
Bolwig, T.G., Hansen, E.S., Hansen, A., Merkin, H., Prichep, L.S., 2007. Toward a better understanding of the pathophysiology of OCD SSRI responder: QEEG source localization. Acta Psychiatr. Scand. 115 (3), 237–242.
Bosch-Bayard, J., Valdes-Sosa, P., Virues-Alba, T., Aubert-Vazquez, E., John, E.R., Harmony, T., Riera-Diaz, J., Trujillo-Barreto, N., 2001. 3D statistical parametric mapping of EEG source spectra by means of variable resolution electromagnetic tomography (VARETA). Clin. Electroencephalogr. 32, 47–61.
Bosch-Bayard, J., Galán-García, L., Fernandez, T., Biscay Lirio, R., Roca-Stappung, M., Ricardo-Garcell, J., Harmony, T., Valdes-Sosa, P., 2018. Stable sparse classifiers identify qEEG signatures that predict learning disabilities (NOS) severity. Front. Neurosci. http://dx.doi.org/10.3389/fnins.2017.00749.
Boylan, K., Vaillancourt, T., Boyle, M., Szatmari, P., 2007. Comorbidity of internalizing disorders in children with oppositional defiant disorder. Eur. Child Adolesc. Psychiatry 16 (8), 484–494. http://dx.doi.org/10.1007/s00787-007-0624-1.
Bush, G., Frazier, J.A., Rauch, S.L., Seidman, L.J., Whalen, P.J., Jenike, M.A., Rosen, B.R., Biederman, J., 1999. Anterior cingulate cortex dysfunction in attention deficit/hyperactivity disorder revealed by fMRI and the counting Stroop. Biol. Psychiatry 45, 1542–1552.
Calzada-Reyes, A., Alvarez-Amado, a., Galán-García, L., Valdés-Sosa, M., 2016. QEEG and LORETA in teenagers with conduct disorder and psychopathic traits. In: Clinical EEG and Neuroscience 1–11 © EEG and Clinical Neuroscience Society (ECNS) 2016, 10.1177/1550059416645712. gepub.com/journals Permissions.nav.
Casanova, R., Whitlow, C.T., Wagner, B., Williamson, J., Shumaker, S.A., Maldjian, J.A., Espeland, M.A., 2011. High dimensional classification of structural MRI Alzheimer's disease data based on large scale regularization. Front. Neuroinform. 5, 22. http://dx.doi.org/10.3389/fninf.2011.00022.eCollection.
Castellanos, F.X., Giedd, J.N., Eckburg, P., Marsh, W.L., Vaituzis, C., Kaysen, D., Hamburger, S.D., Rapoport, J.L., 1994. Quantitative morphology of the caudate nucleus in attention deficit hyperactivity disorder. Am. J. Psychiatry 151, 1791–1796.
Castellanos, F.X., Giedd, J.N., Marsh, W.L., Hamburger, S.D., Vaituzis, A.C., Dickstein, D.P., Sarfatti, S.E., Vauss, Y.C., Snell, J.W., Lange, N., Kaysen, D., Krain, A.L., Ritchie, G.F., Rajapakse, J.C., Rapoport, J.L., 1996. Quantitative brain magnetic resonance imaging in attention-deficit hyperactivity disorder. Arch. Gen. Psychiatry 53, 607–616.
Chabot, R.J., Merkin, H., Wood, L.M., Davenport, T.L., Serfontein, G., 1996. Sensitivity and specificity of qEEg in children with attention deficit or specific developmental learning disorders. Clin. Electroencephalogr. 27, 26–34.
Chabot, R.J., Orgill, A.A., Crawford, G., Harris, M.J., Serfontein, G., 1999. Behavioral and electrophysiologic predictors of treatment response to stimulants in children with attention disorders. J. Child Neurol 14 (6), 343–351.
Chabot, R.J., di Michele, F., Prichep, L.S., John, E.R., 2001. The clinical role of computerized EEG in the evaluation and treatment of learning and attention disorders in children and adolescents. J. Neuropsychiatry Clin. Neurosci. 13 (2), 171–186.
Chabot, R.J., Coben, R., Hirshberg, L., Cantor, D.S., 2015. QEEG and VARETA based neurophysiological indices of brain dysfunction in attention deficit and autistic spectrum disorder. Austin J. Autism Relat. Disabilities 1 (2), 1–8.
Clarke, A.R., Barry, R.J., McCarthy, R., Selikowitz, M., 2001. Excess beta in children with attention-deficit/hyperactivity disorder: an atypical electrophysiological group. Psychiatry Res. 103, 205–2018.
Clarke, A.R., Barry, R.J., McCarthy, R., Selikowitz, M., 2002. Children with attention-deficit/hyperactivity disorder and comorbid oppositional defiant disorder: an EEG analysis. Psychiatry Res. 111, 181–190.
Cloninger, C.R., 1998. The genetics and psychobiology of the seven factor model of personality. In: Silk, K.R. (Ed.), Biology of Personality Disorder. American Psychiatric Press, Washington, DC, pp. 63–92.
Cloninger, C.R., 2002. Functional neuroanatomy and brain imaging of personality and its disorders. In: D'haenen, H., den Boer, J.A., Willner, P. (Eds.), Biological Psychiatry. XXVI-6. John Wiley Sons, Ltd., pp. 1–9.
Cloninger, C.R., 2004. Feeling Good: The Science of Well-Being. Oxford University Press.
Cloninger, C.R., Svrakic, D.M., 2000. Personality disorders. In: Sadock, B.J., Sadock, V.A. (Eds.), Comprehensive Textbooks of Psychiatry (7th edn) pp. Lippincott Williams & Wilkins, New York, pp. 1723–1764.
Cloninger, C.R., Svrakic, D.M., Przybeck, T.R., 1993. A psychobiological model of temperament and character. Arch. Gen. Psychiatry 50, 975–989.
Cloninger, C.R., Przybeck, T.R., Svrakic, D.M., Wetzel, R.D., 1994. The Temperament and Character Inventory (TCI): A Guide to its Development and Use. Washington University Center for Psychobiology of Personality, St. Louis, MO.
Conners, C.K., 1997. Conners' Rating Scales-Revised, Technical Manual. MultiHealth Systems Inc, Toronto.
Cornoldi, C., Gardinale, M., Pettenò, L., Masi, A., 1996. Impulsività e Autocontrollo, Interventi e Tecniche Metacognitive, Trento: Erickson.
Corsi-Cabrera, M., Figueredo-Rodríguez, P., del Río-Portilla, Y., Sánchez-Romero, J., Galán, L., Bosch-Bayard, J., 2012. Enhanced frontoparietal synchronized activation during the wake-sleep transition in patients with primary insomnia. Sleep 35 (4), 501–511. http://dx.doi.org/10.5665/sleep.1734. 2012 Apr 1.
Cortese, S., Kelly, C., Chabernaud, C., Proal, E., Di Martino, A., Milham, M.P., Castellanos, F.X., 2012. Toward systems neuroscience of ADHD: a meta-analysis of 55 fMRI studies. Am. J. Psychiatry 169, 1038–1055.
Damasio, A.R., 1985. The frontal lobes. In: Heilman, K.M., Valenstein, E. (Eds.), Clinical Neuropsychology. Oxford University Press, New York, pp. 339–375.
Donfrancesco, R., Di Trani, M., Porfirio, M.C., Giana, G., Miano, S., Andriola, E., 2015. Might the temperament be a bias in clinical study on attention-deficit hyperactivity disorder (ADHD)? Novelty Seeking dimension as a core feature of ADHD. Psychiatry Res. 227 (2–3), 333–338. http://dx.doi.org/10.1016/j.psychres.2015.02.014. (Epub 2015 Feb 27).
Ernst, M., Nelson, E.E., McClure, E.B., Monk, C.S., Munson, S., Eshel, N., Zarahn, E., Leibenluft, E., Zametkin, A., Towbin, K., Blair, J., Charney, D., Pine, D.S., 2004. Choice selection and reward anticipation: an fMRI study. Neuropsychologia 42 (12), 1585–1597.
Evans, A.C., Collins, D.L., Mills, S.R., Brown, E.D., Kelly, R.L., Peters, T.M., 1993. In: 3D Statistical Neuroanatomical Models from 305 MRI Volumes. Proceedings of IEEE-Nuclear Science Symposium and Medical Imaging Conference. 95. pp. 1813–1817.
Evans, A.C., Collins, D.L., Neelin, P., MacDonald, D., Kamber, M., Marrett, T.S., 1994. Three-Dimensional correlative imaging: applications in human brain mapping. In: Thatcher, R., Hallet, M., Zeffiro, T., John, E.R., Huerta, M. (Eds.), Functional Neuroimaging: Technical Foundations. Academic Press, New York, pp. 145–161.
Friedman, J., Hastie, T., Tibshirani, R., 2008. Regularization paths for generalized linear models via coordinate descent. J. Stat. Softw. 33 (1) 1–22 Feb 2010. http://www.jstatsoft.org/v33/i01/.
Fuster, J.M., 1997. The Prefrontal Cortex: Anatomy, Physiology, and Neuropsychology of Frontal Lobes. Lippincott-raven, New York.
Gardini, S., Cloninger, C.R., Venneri, A., 2009. Individual differences in personality traits reflect structural variance in specific brain regions. Brain Res. Bull. 79, 265–270.
Gasser, T., Bacher, P., Mochs, J., 1982. Transformation towards the normal distribution of broad band spectral parameters of the EEG. EEG Clin. Neurophysiol. 53, 119–124.
Gaub, M., Carlson, C.L., 1997. Behavioral characteristics of DSM-IV ADHD subtypes in a school-based population. J. Abnorm. Child Psychol. 25, 103–111.
Gillespie, N.A., Cloninger, C.R., Heath, A.C., Martin, N.G., 2003. The genetic and environmental relationship between Cloninger's dimensions of temperament and character. Pers. Individ. Diff. 35 (8), 1931–1946.
Goel, V., Gold, B., Kapur, S., Houle, S., 1997. The seats of reason? An imaging study of deductive and inductive reasoning. Neuroreport 8 (5), 1305–1310.
Goodyear, P., Hynd, G., 1992. Attention deficit disorder with (ADDH) and without (ADDWO) hyperactivity, behavioral and neuropsychological differentiation. J. Clin. Child Psychol. 21, 273–304.
Gusnard, D.A., Akbudak, E., Shulman, G.L., Raichle, M.E., 2001. Medial prefrontal cortex and self-referential mental activity: relation to a default mode of brain function. Proc. Natl. Acad. Sci. U.S.A. 98 (7), 4259–4264 (Epub 2001 Mar 20).
Gusnard, D.A., Ollinger, J.M., Shulman, G.L., Cloninger, C.R., Price, J.L., Van Essen, D.C., Raichle, M.E., 2003. Persistence and brain circuitry. Proc. Natl. Acad. Sci. U. S. A. 100 (6), 3479–3484.
Hamilton, S.S., Armando, J., 2008. Oppositional defiant disorder. Am. Fam. Physician 78 (7), 861–866.
Hastings, J., Barkley, R.A., 1978. A review of psychophysiological research with hyperactive children. J. Abn. Child Psychol. 7, 337–413.
Hernandez-Gonzales, G., Bringas-Vega, M.L., Galán-Garcia, L., Bosch-Bayard, J., Lorenzo-Ceballos, Y., Melie-Garcia, L., Valdes-Urrutia, L., Cobas-Ruiz, M., Valdes-Sosa, P.A., 2011. Multimodal quantitative neuroimaging databases and methods: the Cuban human brain mapping project. Clin EEG Neurosci. 42 (3), 149–159.
Jaworska, N., Berrigan, L., Ahmed, A.G., Gray, J., Korovessis, A., Fisher, D.J., Bradford, J., Federoff, P., Knott, V.J., 2013. The resting electrophysiological profile in adults with ADHD and comorbid dysfunctional anger: a pilot study. Clin. EEG Neurosci. 44, 95–104.
John, E.R., Ahn, H., Prichep, L.S., Trepetin, M., Brown, D., Kaye, H., 1980. Developmental equations for the electroencephalogram. Science 210, 1255–1258.
John, E.R., Prichep, L.S., Ahn, H., Easton, P., Friedman, J., Kaye, H., 1983. Neurometric evaluation of cognitive dysfunctions and neurological disorders in children. Prog. Neurobiol. 21, 239–290.
John, E.R., Prichep, L.S., Friedman, J., Easton, P., 1988. Neurometrics: computer-assisted differential diagnosis of brain dysfunctions. Science 293, 162–169.
Joseph, R., 1999. Frontal lobe psychopathology: mania, depression, confabulation, perseveration, obsessive compulsions, and schizophrenia. Psychiatry 62, 138–172.
Kelly, D., 1980. Anxiety and emotions: Physiological Basis and Treatment. Charles C. Thomas, Springfield, IL.
Kelly, D., Richardson, A., Mitchell-Heggs, N., 1973. Stereotactic limbic leucotomy: neurophysiological aspects and operative techniques. Brit. J. Psych. 123, 133–140.
Kim, H.W., Cho, S.C., Kim, B.N., Kim, J.W., Shin, M.S., Yeo, J.Y., 2010. Does oppositional defiant disorder have temperament and psychopathological profiles independent of attention deficit/hyperactivity disorder? Compr. Psychiatry 51 (4), 412–418. Jul-Aug. https://doi.org/10.1016/j.comppsych.2009.09.002 (Epub 2009 Dec 21).
Kim, K.M., Nam, S., Kim, S.Y., Lee, S.M., Choi, J.W., Kang, T., Kim, J.W., 2017. Psychopathological, temperamental, and characteristic factors in adults with remaining childhood attention-deficit hyperactivity symptoms. Int. J. Psychiatry Clin. Pract. 7, 1–6. http://dx.doi.org/10.1080/13651501.2017.1297835.
Klorman, R., 1992. Cognitive event-related potentials in attention deficit disorder. In: Shaywitz, S.E., Shaywitz, B.A. (Eds.), Attention Deficit Disorder Comes of Age: Toward the Twenty-First Century. Pro-Ed., Austin, TX, pp. 221–244.
Knauff, M., Mulack, T., Kassubek, J., Salih, H.R., Greenlee, M.W., 2002. Spatial imagery in deductive reasoning: a functional MRI study. Brain Res. Cogn. Brain Res. 13 (2), 203–212.
Kondacs, A., Szabo, M., 1999. Long-term intra-individual variability of the background EEG in normals. Clin. Neurophysiol. 110, 1708–1716.
Kringelbach, M.L., 2005. The orbitofrontal cortex: linking reward to hedonic experience. Nature Rev. Neurosci. 6, 691–702. http://dx.doi.org/10.1038/nrn1747. (PMID 16136173).
Kringelbach, M.L., Rolls, E.T., 2004. The functional neuroanatomy of the human orbitofrontal cortex: evidence from neuroimaging and neuropsychology. Prog. Neurobiol.

72 (5), 341–372. http://dx.doi.org/10.1016/j.pneurobio.2004.03.006. (PMID 15157726).
Kübler, A., Dixon, V., Garavan, H., 2006. Automaticity and reestablishment of executive control-an fMRI study. J. Cogn. Neurosci. Aug 18 (8), 1331–1342.
Lane, R.D., Reiman, E.M., Axelrod, B., Yun, L.S., Holmes, A., Schwartz, G.E., 1998. Neural correlates of levels of emotional awareness. Evidence of an interaction between emotion and attention in the anterior cingulate cortex. J. Cogn. Neurosci. 10 (4), 525–535.
Loeber, R., Burke, J.D., Lahey, B.B., Winters, A., Zera, M., 2000. Oppositional defiant and conduct disorder: a review of the past 10 years, part I. J. Am. Acad. Child Adolesc. Psychiatry 39 (12), 1468–1484. http://dx.doi.org/10.1097/00004583-200012000-00007.
Loeber, R., Burke, J., Pardini, D.A., 2009. Perspectives on oppositional defiant disorder, conduct disorder, and psychopathic features. J. Child Psychol. Psychiatry 50 (1–2), 133–142. http://dx.doi.org/10.1111/j.1469-7610.2008.02011.x. (Research Support, N.I.H., Extramural Review).
London, E.D., Ernst, M., Grant, S., Bonson, K., Weinstein, A., 2000. Orbito frontal cortex and human drug abuse: functional imaging. Cereb. Cortex 10, 334–342.
Lopez-Larson, M.P., Bradford King, J., Terry, J., McGlade, M.C., Yurgelun-Todd, B., 2012. Reduced insular volume in attention deficit hyperactivity disorder. Psychiatry Res. Neuroimaging 204 (1), 32–39.
Lou, H.C., Henriksen, L., Bruhn, P., 1984. Focal cerebral hypoperfusion in children with dysphasia and/or attention deficit disorder. Arch. Neurol. 41, 825–829.
Lou, H.C., Henriksen, L., Bruhn, P., Borner, H., Nielsen, J.B., 1989. Striatal dysfunction in attention deficit and hyperkinetic disorder. Arch. Neurol. 46, 48–52.
MacLean, P.D., 1958. The limbic system with respect to self-preservation and the preservation of the species. J. Nerv. Ment. Dis. 127, 1–11.
MacLean, P.D., 1962. New finding relevant to the evolution of psycho-sexual functions of the brain. J. Nerv. Ment. Dis. 135, 289–301.
MacLean, P.D., 1990. The Triune Brain in Evolution: Role in Paleocerebral Functions. Plenum Press, New York.
Melegari, M.G., Nanni, V., Lucidi, F., Russo, P.M., Donfrancesco, R., Cloninger, C.R., 2015. Temperamental and character profiles of preschool children with ODD, ADHD, and anxiety disorders. Compr. Psychiatry 58, 94–101. http://dx.doi.org/10.1016/j.comppsych.2015.01.001. (Epub 2015 Jan 8).
di Michele, F., Prichep, L.S., John, E.R., Chabot, R.J., 2005. The neurophysiology of attention-deficit/hyperactivity disorder. Int. J. Psychophysiol. 58, 81–93.
Mulert, C., Pogarell, O., Juckel, G., Rujescu, D., Giegling, I., Rupp, D., Mavrogiorgou, P., Bussfeld, P., Gallinat, J., Möller, H.J., Hegerl, U., 2004. The neural basis of the P300 potential: focus on the time-course of the underlying cortical generators. Eur. Arch. Psychiatry Clin. Neurosci. 254, 190–198.
Nauta, W.J.H., 1971. The problem of the frontal lobe: a reinterpretation. J. Psych. Res. 8, 167–187.
Noordermeer, S.D.S., Luman, M., Oosterlaan, J., 2016. A systematic review and meta-analysis of neuroimaging in oppositional defiant disorder (ODD) and conduct disorder (CD) taking attention-deficit hyperactivity disorder (ADHD) into account. Neuropsychol. Rev. 26, 44–72. http://dx.doi.org/10.1007/s11065-015-9315-8.
Papez, J.W., 1937. A proposed mechanism of emotion. Arch. Neurogy Psychiatry 38, 725–743.
Park, H., Suh, B.S., Lee, H.K., Lee, K., 2016. Temperament and characteristics related to attention deficit/hyperactivity disorder symptoms. Compr. Psychiatry 112–117. http://dx.doi.org/10.1016/j.comppsych.2016.07.003. (Epub 2016 Jul 6).
Pascual-Marqui, R.D., Valdes-Sosa, P.A., Alvarez-Amador, A., 1998. A parametric model for multichannel EEG spectra. Int. J. Neurosci. 40 (1–2), 89–99.
Paulus, M.P., Hozack, N.E., Zauscher, B.E., Frank, L., Brown, G.G., Braff, D.L., Schuckit, M.A., 2002. Behavioral and functional neuroimaging evidence for prefrontal dysfunction in methamphetamine-dependent subjects. Neuropsychopharmacology 26 (1), 53–63. http://dx.doi.org/10.1016/s0893-133x(01)00334-7.
Prichep, L.S., John, E.R., Tom, M.L., 2001. Localization of deep white matter lymphoma using VARETA - a case study. Clin. EEG 32 (2), 62–66.
Riera, J.J., Fuentes, M.E., 1998. Electric lead field for a piecewise homogeneous volume conductor model of the head. IEEE Trans. Biomed. Eng. 45 (6), 746–753.
Rogers, R.D., Owen, A.M., Middleton, H.C., Williams, E.J., Pickard, J.D., Sahakian, B.J., Robbins, T.W., 1999. Choosing between small, likely rewards and large, unlikely rewards activates inferior and orbital prefrontal cortex. J. Neurosci. 19 (20), 9029–9038.
Rubia, K., Overmeyer, S., Taylor, E., Brammer, M., Williams, S.C.R., Simmons, A., Bullmore, E.T., 1999. Hypofrontality in attention deficit hyperactivity disorder during higher-order motor control, a study with functional MRI. Am. J. Psychiatry 156, 891–896.
Rubia, K., Taylor, E., Smith, A.B., Oksannen, H., Overmeyer, S., Newman, S., 2001. Neuropsychological analyses of impulsiveness in childhood hyperactivity. Br. J. Psychiatry 179, 138–143.
Rubia, K., Halari, R., Cubillo, A., Mohammed, A.M., Brammer, M., Taylor, E., 2011. Methylphenidate normalizes fronto-striatal underactivation during interference inhibition in medication-nave boys with attention-deficit hyperactivity disorder. Neuropsychopharmacology 36, 1575–1586.
Russell-Chapin, L., Kemmerly, T., Liu, W.C., Zagardo, M.T., Chapin, T., Dailey, D., Dinh, D., 2013. The effects of neurofeedback in the default mode network: pilot study results of medicated children with ADHD. J. Neurother. 17 (1), 35–42.
Schoenbaum, G., Takahashi, Y., Liu, T., McDannald, M., 2011. Does the orbitofrontal cortex signal value? Ann. N. Y. Acad. Sci. 1239, 87–99. http://dx.doi.org/10.1111/j.1749-6632.2011.06210.
Schultz, W., Tremblay, L., Hollerman, J.R., 1998. Reward prediction in primate basal ganglia and frontal cortex. Neuropharmacology 37, 421–429.
Soloff, P.H., Meltzer, C.C., Greer, P.J., Constantine, D., Kelly, T.M., 2000. A fenfluramine-activated FDG-PET study of borderline personality disorder. Biol. Psychiatry 47, 540–547.
de Sonneville, L.M.J., 2014. Handbook Amsterdam Neuropsychological Tasks. Boom Test Publishers, Amsterdam.
Sugiura, M., Kawashima, R., Nakagawa, M., Okada, K., Sato, T., Goto, R., Sato, K., Ono, S., Schormann, T., Zilles, K., Fukuda, H., 2000. Correlation between human personality and neural activity in cerebral cortex. NeuroImage 11 (5 Pt 1), 541–546.
Swanson, J., 1992. School-Based Assessment and Interventions for ADD - Irvine. KC Publishing.
Szatmari, P., 1992. The epidemiology of attention-deficit hyperactivity disorders. In: Weiss, G. (Ed.), Child and Adolescent Psychiatry Clinics of North America: Attention Deficit Disorder. Saunders, Philadelphia, pp. 361–372.
Szava, S., Valdes, P., Biscay, R., Galan, L., Bosch, J., Clark, I., Jimenez, J.C., 1993. High resolution quantitative EEG analysis. Brain Topogr. Spring 6 (3), 211–219.
Taylor, E.A., 1986. The Overactive Child. Lippincott, Philadelphia.
The MTA cooperative group, 1999. A 14-month randomized clinical trial of treatment strategies for attention-deficit/hyperactivity disorder. The MTA cooperative group multimodal treatment study of children with ADHD. Arch. Gen. Psychiatry 56, 1073–1086.
Toplak, M.E., Jain, U., Tannock, R., 2005. Executive and motivational processes in adolescents with attention-deficit-hyperactivity disorder (ADHD). Behav. Brain Funct. 1, 8–20.
Valdes-Sosa, P., Biscay-Lirio, R., Galán-García, L., Bosch-Bayard, J., Szava, S., Virues-Alba, T., 1990. High resolution spectral EEG norms for topography. Brain Topogr. 3 (2), 281–282.
Vedeniapin, A.B., Anokhin, A.A., Sirevaag, E., Rohrbaugh, J.W., Cloninger, C.R., 2001. Visual P300 and the self-directedness scale of the temperament-character inventory. Psychiatry Res. 101, 145–146.
Verdejo-Garcia, A., Bechara, A., Recknor, E.C., Perez-Garcia, M., 2006. Executive dysfunction in substance dependent individuals during drug use and abstinence: an examination of the behavioral, cognitive and emotional correlates of addiction. J. Int. Neuropsychol. Soc. 12, 405–415. http://dx.doi.org/10.1017/s1355617706060486. (PMID 16903133).
Weiss, S.M., Indurkhya, N., 1998. Predictive Data Mining: A Practical Guide. Morgan Kaufmann Publishers.
Westlye, L.T., Bjørnebekk, A., Grydeland, A., Fjell, A.M., Walhovd, K.B., 2011. Linking an anxiety-related personality trait to brain white matter microstructure. Diffusion tensor imaging and harm avoidance. Arch. Gen. Psychiatry 68 (4), 369–377.
Wolosin, S.M., Richardson, M.E., Hennessey, J.G., Denckla, M.B., Mostofsky, S.H., 2009. Abnormal cerebral cortex structure in children with ADHD. Hum. Brain Mapp. 30 (1), 175–184. http://dx.doi.org/10.1002/hbm.20496.
Worsley, K.J., Marrett, S., Neelin, P., Evans, A.C., 1995. A unified statistical approach for determining significant signals in location and scale space images of cerebral activation. In: Myers, R., Cunningham, V.G., Bailey, D.L., Jones, T. (Eds.), Quantification of Brain Function Using PET. Academic Press, San Diego, pp. 327–333.
Yamasue, H., Abe, O., Suga, M., Yamada, H., Rogers, M.A., Aoki, S., Kato, N., Kasai, K., 2008. Sex-linked neuroanatomical basis of human altruistic cooperativeness. Cereb. Cortex 18, 2331–2340.
Zumsteg, D., Wennberg, R.A., Treyer, V., Buck, A., Wieser, H.G., 2005. H2(15)O or 13NH3 PET and electromagnetic tomography (LORETA) during partial status epilepticus. Neurology 65, 1657–1660.

brain sciences

MDPI

Article

Clinical and Electrophysiological Differences between Subjects with Dysphonetic Dyslexia and Non-Specific Reading Delay

Jorge Bosch-Bayard [1], Valeria Peluso [2], Lidice Galan [3], Pedro Valdes Sosa [4] and Giuseppe A. Chiarenza [2,*]

1 Institute of Neurobiology, UNAM, Mexico City 76230, Mexico; oldgandalf@gmail.com
2 Centro Internazionale dei disturbi di apprendimento, attenzione e iperattività, (CIDAAI) Milano 20125, Italy; valeria.peluso@hotmail.it
3 Cuban Neuroscience Center Havana, Havana 10500, Cuba; lidicegalan2000@yahoo.com
4 MOE Key Lab for Neuroinformation, University of Electronic Science and Technology of China UESTC, Chengdu 610054, China; pedro.valdes.sosa@gmail.com
* Corresponence: giuseppe.chiarenza@fastwebnet.it; Tel.: +39-348-770-3089

Received: 1 August 2018; Accepted: 7 September 2018; Published: 10 September 2018

Abstract: Reading is essentially a two-channel function, requiring the integration of intact visual and auditory processes both peripheral and central. It is essential for normal reading that these component processes go forward automatically. Based on this model, Boder described three main subtypes of dyslexia: dysphonetic dyslexia (DD), dyseidetic, mixed and besides a fourth group defined non-specific reading delay (NSRD). The subtypes are identified by an algorithm that considers the reading quotient and the % of errors in the spelling test. Chiarenza and Bindelli have developed the Direct Test of Reading and Spelling (DTRS), a computerized, modified and validated version to the Italian language of the Boder test. The sample consisted of 169 subjects with DD and 36 children with NSRD. The diagnosis of dyslexia was made according to the DSM-V criteria. The DTRS was used to identify the dyslexia subtypes and the NSRD group. 2–5 min of artefact-free EEG (electroencephalogram), recorded at rest with eyes closed, according to 10–20 system were analyzed. Stability based Biomarkers identification methodology was applied to the DTRS and the quantitative EEG (QEEG). The reading quotients and the errors of the reading and spelling test were significantly different in the two groups. The DD group had significantly higher activity in delta and theta bands compared to NSRD group in the frontal, central and parietal areas bilaterally. The classification equation for the QEEG, both at the scalp and the sources levels, obtained an area under the robust Receiver Operating Curve (ROC) of 0.73. However, we obtained a discrimination equation for the DTRS items which did not participate in the Boder classification algorithm, with a specificity and sensitivity of 0.94 to discriminate DD from NSRD. These results demonstrate for the first time the existence of different neuropsychological and neurophysiological patterns between children with DD and children with NSRD. They may also provide clinicians and therapists warning signals deriving from the anamnesis and the results of the DTRS that should lead to an earlier diagnosis of reading delay, which is usually very late diagnosed and therefore, untreated until the secondary school level.

Keywords: direct test of reading and spelling (DTRS); dysphonetic dyslexia; non-specific reading delay; QEEG; quantitative EEG tomography; source localization, VARETA, Biomarkers

1. Introduction

In 1973, Boder [1] claimed that reading is essentially a two-channel function, requiring the integration of intact visual and auditory processes both peripheral and central. It is essential for normal reading that these component processes go forward automatically. Based on this model, Boder and Jarrico [2] have developed a diagnostic screening procedure which identifies three main subtypes of dyslexia: dysphonetic dyslexia (DD), dyseidetic and mixed, besides a fourth group defined non-specific reading delay (NSRD). The identification of this further subgroup has evident clinical implications for diagnosis, therapy and prognosis. These subgroups are identified by an algorithm that considers the reading quotient and the percentage of errors of the spelling test. An Italian computerized version of the Boder test [2], the Direct Test of Reading and Spelling (DTRS) adapted and validated to Italian language, was developed by Chiarenza and Bindelli [3]. Luisi and Ruggerini [4] and Chiarenza and Di Pietro [5] using the DTRS, have shown that these subtypes of dyslexia and NSRD group exist also in Italian speakers and have almost the same prevalence as seen in dyslexics English-speaking subjects [2,6–8]. An indirect confirmation of the validity of Boder's model has come from the study of information processing time through cognitive brain potentials. In dyslexic subjects, a disproportionate asynchrony exists between the auditory and visual system in the cross-modal processing of auditory and visual information [9,10].

EEG abnormalities in children with learning disabilities have been reported since long time. In a review paper, Chabot et al. [11] have summarized a variety of EEG abnormalities in individuals with dyslexia and related disorders, including poor EEG rhythm, low-voltage background rhythms [12] and increased generalized slowing [13]. However, the clinical utility of these findings has been questioned due to a lack of specificity [14]. Two subsequent studies provided more clinically relevant information [13,15]. EEG abnormalities were found in 24.6% of a sample of 61 children with learning disorders and in only 3.3% of control subjects. Abnormalities in children with learning disorders included increased high amplitude atypical alpha, abnormal focal paroxysmal activity, excess focal delta, persistent delta asymmetry, and excessive EEG response to hyperventilation. These abnormalities were most likely to occur in those LD children with significant pre- and/or postnatal risk factors for brain injury [15,16]. Thus, EEG studies indicate that specific developmental disorders are associated with abnormal EEGs in 25% to 43.5% of these children, with EEG slowing the most common abnormality reported.

Specific learning disabilities have been also extensively studied with new neuroimaging techniques: QEEG, functional Magnetic Resonance Imaging (fMRI), Single Photon Emission Computed Tomography (SPECT), and Diffusion Tensor Imaging (DTI). A variety of structural and functional connectivity abnormalities in patients with dyslexia has been identified [17–19]. Using DTI it has been reported that the degree of myelination in left hemisphere cortico-cortical tracts correlates positively with reading skill [20,21] and reduced myelination in left hemisphere white matter tracts connecting inferior frontal, temporal, occipital, and parietal regions has been described among adults with a history of reading disability [22]. Both increased and decreased anatomical using DTI and functional connectivity (task-related fMRI) within the reading network of dorsal and ventral brain regions have been reported in adults with reading difficulties compared to normal readers [23–26].

Since the pioneer work of John et al. [27] and Duffy et al. [28], QEEG abnormalities in both hemispheres have been reported in dyslexic children at rest as well as during complex testing. John (1981) [29] found abnormal QEEGs present in 32.7% of the children with Specific Learning Disorder (SLD) and 38.1% of the children with learning disorder (LD) groups, whereas only 5.5% of an independent sample of normal children had abnormal QEEGs. Discriminant analyses using six multivariate features resulted in 80% correct classification of normal children (87% replication) and 72% correct classification of LD children (65% replication). Using similar neurometric techniques, Marosi et al. [30,31], John and Prichep [32] have further elucidated the nature of neurophysiological abnormality in children with documented learning disorders. Children with learning disorders were shown to have different patterns of brain maturation than normal control subjects. Normal subjects,

with increased age show an increase of posterior/vertex EEG coherence and a decrease in coherence in frontal areas. Increased differentiation of frontal cortical regions, with age, leads to increased communication across basic sensory and association cortex. These systematic maturational changes are often not seen in children with learning disorders. Instead, they show no change in posterior/vertex coherence with age, and levels of frontal coherence remain high across all ages, suggesting a deviation from normal development rather than a maturational lag [30,33]. More recently, abnormally high activity in the delta and theta band has been reported in a group of children with learning disabilities not otherwise specified (LD-NOS) who had low scores in reading, writing and calculation tests [34,35]. Flynn and Deering [36] and Flynn et al. [37], using the Boder test classification [2], investigated whether electrophysiological evidence among dyslexic subgroups, could be demonstrated by analysis of QEEG patterns during school-related tasks. The authors found increased left temporo-parietal theta activity in dyseidetic children assuming an overuse of the left-language system activation in patients with visuo-spatial problems recognition.

Other neuroimaging studies using reading-related potentials recorded during reading aloud self-paced single-letter showed that children with DD had abnormal activation at short latencies in the left temporal polar area, at middle latencies in the temporal polar and inferior frontal regions bilaterally and at long latencies in fronto-temporal regions of the right hemisphere [38]. This indicates an early involvement of frontal regions during reading and it may be related to a significantly higher activation of the right hemisphere. This would seem very likely to be related to compensatory mechanisms adopted by reading-impaired children to improve their performance. On the contrary, impaired neural activation of the dyslexic group was present in the left and medial parietal regions: at short and middle latencies, it was present in the angular and then in the supramarginal gyrus; at long latencies, it moved in the middle precuneus and occipital lobe. Therefore, behavioral signs of reading impairment can be related to reduced activation in the left dorsal parieto-occipital regions that have been shown to be specifically involved in reading processes and particularly in the storage and processing of the visual and auditory representations of alphabetic characters [39]. These results are consistent with previous findings of greater recruitment of cerebral regions in the right hemisphere in dyslexic children in comparison with controls [40].

Although all the cited studies identify the left temporo-parietal region as the region where the greatest differences between normal and dyslexic subjects are found, electrophysiological differences between subtypes of dyslexia according to Boder classification have not been further confirmed also due to different clinical classifications. Furthermore, we are not aware of studies that compare children with different subtypes of dyslexia with children with NSRD using electrophysiological methods.

QEEG can be used to indicate which children with learning problems have a measurable underlying neurophysiological dysfunction and which do not. The purpose of this research was to find differences between DD and NSRD groups, both at the neurophysiological and neuropsychological levels. At the same time, we wanted to find a classification equation which discriminates the two groups with a high percent of accuracy. This could contribute to the earlier diagnosis of the NSRD group, usually very late diagnosed and therefore, untreated until the secondary school level.

2. Materials and Methods

2.1. Subjects (Entire Sample)

Seven-hundred-seventy-onesubjects, 488 males between the ages of 7 and 16 (mean age 9.24; SD 0.9) and 283 females between the ages of 6 and 18 (mean age 8.99.2; SD 1.98) were examined at our center for suspected developmental dyslexia. After administration of the DTRS, 83 subjects were diagnosed as normal (10.7%), 113 subjects had NSRD (14.6%), 394 had DD (51.1%), 43 had dyseidetic dyslexia (5.6%), 107 subjects had mixed dyslexia (13.9%), 31 subjects were remediated (4.0%).

Composition of the Subsample

One-hundred-sixty-nine out of the 394 DD subjects had EEG studies: 13 of them had 2 studies and 2 of them had 3 studies. From the NSRD, 36 out of 113 had EEG studies: 8 of them with 2 studies. Statistical analysis was then performed on 169 DD and 36 subjects with NSRD. Due to the big differences between number of subjects in both groups, a special version of the t-test for non-balanced samples was used.

The gender composition of the EEG subsample was as follows: DD: 110 males between the ages of 7 and 15 (mean age 9.4; SD 1.9) and 59 females between the ages of 7 and 14 (mean age 8.8; SD 1.8); NSRD: 22 males between the ages of 7 and 14 (mean age 9.9; SD 1.9) and 14 females between the ages of 7 and 15 (mean age 9.6; SD 2.4).

2.2. Clinical Protocol

The clinical assessment was conducted according to the following protocol: the parents (one or both) were clinically interviewed to obtain family history and the following information was obtained: demographics, parents qualification, medical and psychiatric history including the presence of language delay or specific language disorders, previous and concomitant medications and the eventual type of speech therapy performed or still in progress and its duration. At the first visit, the informed consent was also obtained from parents/caretaker, adolescents and children after explaining them the purpose and the procedures of the study. Physical and neurological examination, EEG, Amsterdam Neuropsychological Test (ANT) [41], a battery to test executive functions and attention, were carried out in the following visits.

The diagnosis of dyslexia was carried out according to Diagnostic and Statistical Manual of Mental Disorders (DSM-V) [42] criteria with the administration of the following tests: (a) WISC III, (b) reading tests for primary school [43], and for secondary school [44] providing accuracy and speed scores in reading aloud age-normed texts, (c) single word and non-word reading, also providing speed and accuracy scores for each grade: the battery for the assessment of dyslexia and developmental dysortography [45], and (d) the Direct test of Reading and Spelling [3,46]. Test AC-MT 6-11: Test di Valutazione Delle Abilità di Calcolo (AC-MT), a battery for dyscalculia [47,48] or the battery for the assessment of developmental dyscalculia [49] were carried out if the anamnesis indicates difficulties in mathematics. The presence of dysgraphia was assessed with Scala Sintetica per la Valutazione Della Scrittura in Età Evolutiva (BHK) [50] and Batteria per la Valutazione della Scrittura e della Competenza Ortografica (BVSCO) tests [51].

In 48 subjects out of 169, dyslexia was associated with dysortography (28.4%), in 6 subjects with dysgraphia (3.5%), in 8 subjects with dyscalculia (4.7%), and in 14 subjects with dysortography, dysgraphia and dyscalculia (8.3%). Eight DD subjects had a previous diagnosis of Specific Language Disorder (SLD). Of these 8 subjects, five DD children received speech therapy lasting 12–48 months. Of the group of 36 subjects with NSRD, 11 subjects were dysortographic (30.5%), 2 subjects dysgraphic (5.5%), 3 subjects had dyscalculia (8.73%) and 4 subjects had dysortography, dysgraphia and dyscalculia (11.1%). One subject with NSRD had a previous diagnosis of Specific Language Disorder (SLD). No therapy had been prescribed for this subject with NSRD.

The most frequent comorbidity in both groups was Attention Deficit and Hyperactivity Disorder (ADHD). In the DD group, 34 subjects (20.1% of total DD subjects) were affected by ADHD: 16 subjects (47.0%) had ADHD of inattentive subtype, 18 subjects (52.9%) had ADHD of combined subtype. In the group of subjects with NSRD, 12 subjects were affected by ADHD (33.3% of the total subjects with NSRD): 6 subjects had ADHD of inattentive type (50%), 5 subjects had ADHD combined subtype (41.7%) and 1 subject with ADHD not specified (8.3%).

The 169 DD subjects had a mean Full Scale Intelligent Quotient (FSIQ) of 101.4 (SD: 10.9), a mean Verbal Intelligent Quotient (VIQ) of 99.6 (SD: 11.7) and a mean Performance Intelligent Quotient (PIQ) of 103.4 (SD: 12.1). The 36 subjects with NSRD had a mean FSIQ of (105.5(SD: 9.2), mean VIQ of 103.9 (SD: 12.1) and a mean PIQ of 106.6(SD: 10.0).

All subjects had neurological examination within normal limits.

Exclusion Criteria

Presence of documented psychiatric disorders in parents, a documented history of Bipolar disorders, history of psychosis or pervasive developmental disorder, seizure disorder, head injury with loss of consciousness or concussion, migraine, neurological/systemic medical disease (e.g., lupus, diabetes) or history of stroke or arterious-venus malformation or brain surgery were considered an exclusion criterion. Functional comorbidities such as visual or auditory processing problems were documented with IQ testing. The presence of ADHD or mild anxiety disorders were not exclusion criteria.

2.3. The Direct Test Reading and Spelling (DTRS)

The DTRS is self-administered and self-paced [3,46]. The DTRS consists of a reading and spelling test. The reading test has 15 lists. The first four are for the first grade of the primary school; the other 10, two for each grade, for the other five grades and the last one for the sixth grade. Each list consists of 20 words, ordered by increasing difficulty according to numbers of syllables and orthographic difficulties (following this design, a complexity index was constructed, which is explained and used in the statistical section). The subject decides spontaneously by pressing a button with the dominant hand to display on a screen the word to be read aloud. A microphone records the subject's phonogram used to measure the reading time of each word. The words lists are presented in two ways: 'flash' and 'untimed' mode. In 'flash mode' the word appears for 250 ms, which determines the child's *sight vocabulary* (i.e., the words the child recognizes instantly as whole word configuration or gestalts). If he/she recognizes a word within one second, this is recorded as 'word flash correct' (FCOR). If he/she hesitates (i.e.: hem ... hem ... 'ice-cream') or reads the word syllable by syllable, it is classified as 'flash hesitating' (FHESIT) and 'flash syllabicating' (FSILL) respectively. If he misreads the word or does not read it at all the child is asked to try again and, the word appears for 10 s 'untimed mode', which calls upon the child's ability to analyze unfamiliar words phonetically (i.e., his *word analysis-synthesis skills)*. If he identifies the word correctly within 10 s this is recorded as 'word untimed correct' (UCOR). If he misreads the word or reads the word with great difficulty they are recorded as 'word untimed incorrectly read' (UINCOR) or words read with great difficulty (UGDIFF). The words not read are recorded as 'NR'.

Comparison of the number of correctly read words in the 'flash' or 'untimed' mode indicates whether the child is reading through both whole-word gestalt and phonetic analysis or predominantly trough one or other. The highest-grade level at which the child's sight vocabulary includes at least 50 per cent of the word list is considered his reading level (RL). Misreadings are recorded for later evaluation of the child's characteristic errors of the subtype of dyslexia. The description of these typical errors of dysphonetic and dyseidetic dyslexia is reported in Appendix A.1.

The spelling test is complementary to the reading test. It consists of dictating to the subject two lists of ten words each: a list of known words (KW) chosen from the 'sight vocabulary', and a list of unknown words (UW), chosen from those unread or read with great difficulty during 'untimed' mode (i.e., not in sight vocabulary). The examiner notes the number of correctly spelled words in both lists and the type of errors. The description of the spelling errors is reported in Appendix A.2. Analysis of the spelling of 'known words' reveals the child's ability to 'revisualize' the words in his sight vocabulary, and analysis of his list of 'unknown words' reveals his ability to spell words not in his sight vocabulary. Thus, the two spelling lists are designed to tap the central visual and auditory processes necessary for spelling, in the same way that the 'flash' and 'untimed mode' of the reading test tap the central visual and auditory processes necessary for reading.

Two independent researchers conducted both a qualitative and quantitative analysis of the errors of the reading and spelling test of the subjects of the entire sample according to the classification

proposed by Boder [1] with the addition of some errors typical of the Italian language as accents and double letters.

At the end of the reading test the computer automatically provides the reading level ('RL'), the reading age ('RA'), and the reading quotient ('RQ'): the ratio between 'RA' and chronological age (CA) (RQ = (RA/CA) × 100). If the child's overall mental ability is substantially above or below average, this quotient is corrected for mental age (MA) by use of the following formula, RQM = (RA/MA) × 100. The RQC is the reading quotient corrected for mental and chronological age according to the following formula, RQC = (2RA/(MA + CA) × 100.

The computer provides also the number of words read correctly in flash (FCOR) and untimed (UCOR) mode and the average reading time of the words of each list read correctly in 'flash mode" (RTFCOR) and in 'untimed mode' (RTUCOR), the average reading time of the words of each list read after marked hesitation (RTFHESIT), the average reading time of the words of each list read incorrectly (RTINCOR) the average reading time of the words of each list read with great difficulty after one or two attempts (RTUGDIFF (the word is read only partially or with the addition of letters or syllables, or with wrong accent); Reading time consists in the time that elapses between the occurrence of the word on the screen and the start of the pronunciation of the word recorded through the phonogram.

Finally, the identification of the dysphonetic reading-spelling pattern and that one of unspecific reading delay is based on the child's performance in the three basic diagnostic indicators: % of words spelled correctly in the known list, % of words spelled correctly in the unknown list and the reading quotient. The dysphonetic pattern is present when the child has a percentage of words correctly spelled in the two lists less than 70% and a reading quotient greater than 67; the non-specific reading delay pattern is present when the child has a percentage of words correctly spelled in the two lists greater than 70 and a reading quotient of less than 90.

The Complexity Index

To obtain a deeper understanding about the reading differences between the DD and NSRD, the reading time results are evaluated. Since children read different lists and words depending on their age and grade, to make them comparable, a complexity index was created. Each word in the list was divided in % of complexity according to the number of syllables and number of orthographic difficulties. Since each list has 20 words, for all individuals 20 levels of degree of complexity for both flash and untimed mode were created. For each level of this normalized index, the corresponding reading time was considered and both groups were compared.

2.4. Neurophysiologic Assessment

2.4.1. EEG Data Acquisition

The EEG was recorded at 19 leads of the 1020 International Positioning System (S10–20), using Electro-caps referenced to linked earlobes. Twenty minutes of eyes closed resting EEG were recorded. A differential eye channel (diagonally placed above and below the eye orbit) was used for detection of eye movements. All electrode impedances were below 5000 Ohms. The EEG amplifiers were set to a bandpass from 0.5 to 70 Hz (3 dB points). All EEG data were collected on the same digital system to achieve amplifier equivalence. Data were sampled at a rate of 256 Hz with 12-bit resolution. All the patients were recorded in the morning and instructed to keep their eyes closed and stay awake. This allowed to control for drowsiness during EEG recordings and to guarantee similar conditions throughout the different sessions. The technician was also aware of the subject's state to avoid drowsiness. Additionally, patients were monitored with a closed-circuit television system, during the recording.

2.4.2. QEEG at the Scalp

EEG experts visually edited the raw EEG data to select EEG epochs free of either biological (e.g., muscle movement, EMG) as well as non-biological (e.g., electrical noise in the room) artifacts. This was augmented by a computerized artifact detection algorithm. A minimum of 24 epochs of 2.56 minutes of artifact-free data, were selected for each subject and submitted to frequency analysis. The EEG spectra were calculated using the High Resolution Spectral (HRS) model [52–54] for all the channels by means of the Fast Fourier Transform (FFT), in a frequency range from 0.39 Hz to 19.11 Hz, with a frequency resolution of 0.39 Hz. The selection of these frequency parameters was made on the basis that they match the available parameters from the Cuban Normative Database [53] to transform the raw EEG spectra into Z-probabilistic measurements, age corrected. The spectra were Log transformed, to approach them to Gaussianity [55,56] and the Z-transform was calculated against the Cuban Normative Database. Significant test-retest reliability for these measures has been demonstrated [27,57,58].

2.4.3. QEEG Source Analysis (QEEGT)

To obtain the raw spectra at the EEG generators, the Variable Resolution Electrical Tomography (VARETA) method [59] was used for the source localization analysis. Same as with the spectra at the electrodes, the source density localization analysis was performed for frequencies between 0.39 to 19.11 Hz and for all the sources in the cerebral cortex for a grid of 3244 sources. VARETA is an already known technique for estimating the distribution of the primary current in the source generators of EEG data. VARETA is a Discrete Spline Distributed Solution, like LORETA [52]. The spline estimates are the spatially-smoothest solutions compatible with the observed data. VARETA however, adapts to the actual degree of smoothness in each voxel being determined by the data itself, by applying different amounts of spatial smoothing for different types of generators; hence the use of the term variable resolution. Additionally, VARETA allows spatially-adaptive nonlinear estimates of current sources eliminating 'ghost solutions' (artefactual interference patterns) often present in linearly-distributed inverse solutions. Therefore, VARETA produces focal solutions for point sources, as well as distributed solutions for diffuse sources. In addition, VARETA introduced the use of anatomical constraints upon the allowable solutions by introducing a 'gray matter weight' for each voxel. The effect of these weights is to prohibit sources in voxels where the mask is zero (for example, CSF or white matter). To solve the EEG forward problem, a three-concentric spheres Lead Field [60], defined over a grid of 3244 points located in the gray matter of the Montreal Neurological Institute (MNI) template [61] was used to generate the voltage at the 19 electrodes of the 10–20 System.

The average reference was applied to the EEG at each time point for this analysis, as required by VARETA and other inverse solution methods. To make the inverse solution in different subjects comparable for statistics at the sources, the same regularization parameter for all subjects was provided to VARETA, which was obtained from the normative database, and it was also used for the norms calculations. The geometric power was applied to standardize the EEGs by a global scale factor. This factor accounts for individual differences in power values due to skull thickness, hair volume, electrode impedance, and other factors of variance that can affect EEG amplitudes not related to electrophysiological variability [62]. This procedure is described in detail in Bosch-Bayard et al. [59]. The anatomical accuracy of the functional QEEG source localization used in VARETA has been repeatedly confirmed by co-registration with other brain imaging modalities e.g., fMRI [63], positron emission tomography, PET [64,65], and computerized tomography [66]. It has also been used satisfactorily for source localization in psychiatric patients [67].

The selected EEG epochs were submitted to VARETA for the computation of the spectra at the EEG sources, using the 3244 sources provided by the grid defined over the gray matter of the probabilistic MRI Brain Atlas [61,68]. The Lead Field was calculated according to [60], using the standard positions of the International 1020 electrodes positioning system. Using this Lead Field, VARETA was applied to the cross-spectral matrices at the scalp for all frequencies and leads, by applying the methodology

described in Bosch-Bayard et al. [59] to calculate the spectra at the sources space with the same frequency resolution (from 0.39 to 20 Hz with a frequency resolution of 0.39 Hz: high spectral resolution, HSR). The procedure of obtaining the spectra for every source of the gray matter at each frequency constitutes a new type of neuroimaging technique that has been termed Quantitative EEG Tomographic Analysis (QEEGT) [59].

As pointed out above, to account for age differences, the Z-spectra were computed relative to the normative values of the Cuban Normative Database. The values computed for the 3244 sources were encoded using a color palette with hues proportional to the standard- or Z-scores of deviations from expected normative values. The random fields theory [69] was used to correct the significance levels of the images for the large number of comparisons. This approach proposes a unified statistical theory for assessing the significance of apparent signal observed in noisy difference images, giving an estimate of the corrected p-value for local maxima of Gaussian fields over search regions of any shape or size in any number of dimensions.

2.4.4. Stability Based Biomarkers Identification

The methodology used in this paper has been described in detail in Bosch-Bayard et al. [34]. The algorithm is an approach for solving the classification problem that guarantees stability and robustness, a property of great usefulness in problems where the sample is small, and the number of variables is high. The method is divided in two steps, one for the parameter estimation and the other for the validation procedure. In the first step, a random subsample of the original sample is generated using the 30% of the variables and the 70% of the subjects and the classification procedure is applied to this subsample. We use the General Linear Model via elastic net (GLMNet) [70] which is a logistic penalized regression method. This method extracts a sparse subset of classifiers from the whole set of variables, while discarding the rest. The random procedure is repeated a sufficiently number of times (500 times in our case), storing the classifiers in each of them. The variables selected as classifiers in at least 50% of the times that they participated in the classification procedure integrate the final set of biomarkers. To measure the classification power of the selected set of biomarkers, a robust version of the ROC technique is used. In this case, all biomarkers are kept while generating a subsample with about the 70% of the subjects. The ROC area is calculated for the 10, 20 and 100% of False Positive (FP) and these numbers are stored. The procedure is randomly repeated a sufficiently high number of times (500 in our case). Three empirical distributions of the ROC values are obtained for the two levels of FP and the total area. The values of these distributions at the 50% of the curve are given as the stable estimate of area under the ROC, which characterizes the predictive classification power of the selected set of biomarkers.

2.5. Statistical Analyses

Group differences were tested for the DTRS variables as well as the QEEG spectra at the scalp and at the sources by means of the t-Student. To account for the very unbalanced samples, a special algorithm was developed, which also corrected the levels of significance for multi comparisons. The algorithm consisted in generating 100 random subsamples of the DD group, of the same length as the NSRD group and performing t-tests between them. For each repetition the t and the P values were stored, and empirical distributions of the t values were created for all the variables and subsamples. The corrected values at the 0.05 threshold were obtained by taken the t values at the 5% and 95% of the empirical distribution.

Additionally, a classification algorithm for biomarkers detection between the two groups was applied to each dataset [34]: DTRS and the QEEGT spectra at the scalp and at the sources. Since the DTRS is the instrument used in the Boder algorithm to classify the subjects into the DD and NSRD groups, we only included in the biomarkers selection procedure those DTRS items which were not used in the Boder algorithm (% of known words, % of unknown words, RL, RA, RQ, RQM, RQC).

Therefore, in the case of the DTRS data, we found a set of biomarkers completely independent to those used for the creation of the dyslexia subgroups.

3. Results

3.1. Results of the DTRS

From the collection of anamnestic and clinical data, the comparison between the two groups of subjects revealed that the age at the time of DTRS testing was highly significant ($p = 0.0129$, $t = -2.51$). The NSRD were significantly older at the time of testing than the DD children. Sex, FSIQ, VIQ and PIQ, the presence of specific language disorder, the associated diagnosis of dysorthography, dysgraphia, and dyscalculia and parental schooling were not significantly different in the two groups. Also, the presence of speech therapy, the type of speech therapy and its duration was not significantly different between the two groups. Subjects with NSRD had a greater presence of comorbidity than DD subjects, but the type of comorbidity was not significantly different in the two groups (Table 1).

Table 2 shows the results of the reading test of DTRS in the two groups. As well as age at the time of DTRS administration also the school level was significantly different in the two groups. Subjects with NSRD were on a higher school level than DD subjects at the time of testing. The number of lists read by the subjects, the reading level, i.e., the last list where the subjects read less than 50% of the words in flash mode and the reading age were not significantly different in the two groups. The subjects with NSRD had a significant lower RQ, RQM and RQC than the subjects with DD.

Table 1. *t*-test results of the anamnestic data of the two groups: mean, SD, *t* value and *P* value. DD. = Dysphonetic dyslexia, NSRD = Non-Specific Reading Delay, N.S. = number of subjects, SD = standard deviation, FSIQ = full scale intelligent quotient, VIQ = verbal intelligent quotient, PIQ = performance intelligent quotient, S.L.D. = specific language disorder, Dysorth. = Dysorthography, Dysgr. = dysgraphia, Dyscal. = dyscalculia, Com. = comorbidity, T.O.C. = type of comorbidity, S.T. = speech therapy, T.O.S.T. = type of speech therapy, S.T.D. = speech therapy duration, F.Q. = father qualification, M.Q. = mother qualification.

	FSIQ	**VIQ**	**PIQ**	**S.L.D.**	**Dysorth.**	**Dysgr.**	**Dyscal.**	**Com.**	**T.O.C.**	**S.T.**	**T.O.S.T.**	**S.T.D.**	**F.Q.**	**M.Q.**
DD (N.S. = 169)—Means	101.4	99.6	103.4	0.57	0.6	0.21	0.31	0.25	6.48	0.19	0.08	3.36	2.27	2.34
NSRD (N.S. = 36)—Means	105.5	103.9	106.6	0.58	0.49	0.22	0.27	0.44	6.5	0.04	0	0.31	2.38	2.22
DD—SD	10.9	11,7	12,1	0.61	0.49	0.41	0.46	0.43	1.66	0.39	0.5	9.04	2.39	2.36
NSRD—SD	9.2	12.1	10.0	0.54	0.51	0.42	0.45	0.5	0.61	0.21	0	1.47	2.26	2
DD Vs. NSRD—*P* value	0.02	0.03	0,1	0.93	0.18	0.88	0.59	0.008	0.95	0.01	0.29	0.025	0.79	0.75
DD Vs. NSRD—*t* value	−2.3	−2.19	−1.64	−0.08	1.32	−0.14	0.53	−2.7	−0.06	2.4	1.04	2.25	−0.26	0.31

Table 2. Means, SD, *t*-test results of the reading test of DTRS in the two groups. DD = dysphonetic dyslexia, NSRD = Unspecific reading delay, SD=standard deviation, N.L.R. = Number of lists read, RL = reading level, RA = reading age, RQ = reading quotient related to chronological age, RQM = reading quotient related to mental age, RQC = reading quotient related to mental and chronological age.

	School	Age at DTRS	N.L.R.	RL	RA	RQ	RQM	RQC
DD (N.S. = 169)—Means	1.26	10.02	6.72	2.38	8.07	80.58	79.99	80.08
NSRD (N.S. = 36)—Means	1.47	10.84	6.87	2.27	8.12	75.23	71.64	73.26
DD—SD	0.46	1.92	2.49	1.38	1.79	9.63	9.82	8.64
NSRD—SD	0.59	2.17	2.3	1.5	1.82	10.04	9.98	9.52
DD Vs. NSRD—*P* value	0.011	0.013	0.72	0.66	0.88	0.001	7.8×10^{-7}	6.1×10^{-6}
DD Vs. NSRD—*t* value	−2.56	−2.51	−0.36	0.43	−0.15	3.31	5.08	4.64

Table 3 shows the results of the spelling test of DTRS in the two groups. The percentage of known words and unknown words spelled correctly was significantly higher in the NSRD group compared to the DD children. The qualitative and quantitative analysis of the errors of the spelling test showed that the insertion/omission of letters was among the various types of errors (see Appendix A.2) that were significantly different between the two groups. Insertion/omission of letters were significantly higher in DD subjects than subjects with NSRD. In addition, the DD subjects had a total number of errors of dysphonetic and dyseidetic type significantly greater than the NSRD subjects in the list of known words correctly spelled. The DD subjects made a greater number of errors of dysphonetic type compared to the NSRD subjects in the list of unknown words. The most frequent errors made by the DD subjects were accentuation errors, lack of double, insertion/omission of letters, difficulty in the grapheme-phoneme correspondence and grapheme exchange.

Table 4 shows the results of the comparison of the number of words read correctly and incorrectly in flash and untimed mode and their relative reading times between the two groups. The number of words read correctly and incorrectly and their relative reading times in both flash and untimed mode were not significantly different between the two groups. However, it is interesting to report that the only significant difference between the two groups was found in the number of words read in a hesitant way. The NSRD subjects had a significantly greater number of words read in this mode than the DD subjects.

Table 5 shows the t test results of reading times of DD and NSRD groups according to the complexity index by syllables and number of difficulties and by reading mode (flash, untimed).

The most consistent and significant results were found in the reading time of words correctly read and read with evident difficulty in untimed mode. The DD subjects read more slowly than subjects with NSRD when they faced words with a greater number of syllables that also contained a greater number of orthographic difficulties. The greatest differences were found with words of 4 or 5 syllables; however with words of 6 or 7 syllables there were no significant differences between the groups.

Table 3. *t*-test results of the spelling test of the DTRS of the two groups: mean, SD, *t* value and *P* value. N.S. = number of subjects, %KW = % known words, %UW = % unknown words, N.D.E.KW = number of dysphonetic errors of known words, D.E.IOL.UW = dysphonetic errors-insertion/omission of letters of known words, N.DY.E.KW = number of dyseidetic errors of known words, N.D.E.UW = number of dysphonetic errors of unknown words, D.E.MDL.UW = dysphonetic errors of missing double letters of unknown words, D.E.A.UW = dysphonetic errors of accent of unknown words, D.E.GP.UW = dysphonetic errors correspondence grapheme-phoneme of unknown words, D.E.IOL.UW = dysphonetic errors-insertion/omission of letters of unknown words, D.E.MG.UW = dysphonetic errors-mismatch of grapheme of unknown words.

	%KW	%UW	N.D.E.KW	D.E.IOL.KW	N.DY.E.KW	N.D.E.UW	D.E.MDL.UW	D.E.A.UW	D.E.GP.UW	D.E.IOL.UW	D.E.MGUW
DD (N.S. = 169)—Means	71.81	47.65	1.9	1.06	1.2	5.1	1.35	0.28	1.51	1.21	0.56
NSRD (N.S. = 36)—Means	89.44	83.61	0.6	0.29	0.4	1.7	0.3	0.11	0.5	0.55	0.2
DD—SD	18.68	15.5	1.6	1.17	1.4	2.4	1.46	0.53	1.54	1.23	0.13
NSRD—SD	7.43	5.84	0.7	0.51	0.5	1	0.51	0.31	0.64	0.68	0.34
DD Vs. NSRD *P* value	2.8×10^{-10}	1.4×10^{-33}	3.2×10^{-7}	2.4×10^{-5}	1.0×10^{-10}	1.5×10^{-17}	4.8×10^{-6}	0.012	1.2×10^{-5}	0.001	0.008
DD Vs. NSRD *t* value	−6.61	−14.38	5.27	4.31	3.55	9.29	4.69	2.53	4.47	3.3	2.68

Table 4. *t*-test results of the reading test of DTRS of the two groups: mean, SD, *t*-value and *p*-value. SD = standard deviation, FCOR = number of words correctly read in flash mode, FINCORCOR = number of words incorrectly read in flash mode, FHESIT = number of words hesitating read in flash mode, FSILL = number of words syllabicating read in flash mode, UCOR = number of words correctly read in untimed mode, UINCOR = number of words incorrectly read in untimed mode, UGDIFF = number of words read with great difficulty in untimed mode, NR = number of words not read, RTFCOR = averaged reading time of words correctly read in flash mode, RTFINCORCOR = average reading time of words incorrectly read in flash mode, RTFHESIT = average reading time of words hesitating read in flash mode, RTFSILL = average reading time of words syllabicating read in flash mode, RTUCOR = average reading time of words correctly read in untimed mode, RTUINCORCOR = average reading time of words incorrectly read in untimed mode, RTUGDIFF = average reading time of words read whit great difficulty in untimed mode.

	FCOR	FINCOR	FHESIT	FSILL	UCOR	UINCOR	UGDIFF	NR	RTFCOR	RTFINCOR	RTFHESIT	RTFSILL	RTUCOR	RTUINCOR	RTUGDIFF
DD (N.S. = 169)—Means	15.1	2	1.8	0.2	2.7	0.2	0.3	0	1	2	2	1.26	1.6	1.7	3.3
NSRD (N.S. = 36)—Means	14.6	2	3	0.1	2.1	0	0.1	0	1	1,9	1.9	1.84	1.6	2	3.2
DD—SD	4.5	2.2	2.6	0.7	4	0.5	0.8	0.2	0.5	1.1	1	0.77	0.7	1.9	1.9
NSRD—SD	4.2	2.4	4	0.5	2.6	0.2	0.3	0	0.5	1.1	1	0.25	0.9	1.9	1.9
DD Vs. NSRD—*P* value	4.49	0.65	0.01	0.3	0.27	0.12	0.14	0.50	0.33	0.90	0.64	0.22	0.90	0.50	0.70
DD Vs. NSRD—*t* value	4.49	0.46	−2.55	1.05	1.11	1.55	1.49	0.68	0.97	0.12	0.47	−1.25	0.16	−0.68	0.38

Table 5. Significant differences of DD vs. NSRD in reading time according to the reading mode (by columns) compared to the words difficulty (by rows). The rows name indicates: the first digit, the number of syllables of the word and the second digit, the number of grammatical difficulties. By columns: 11: Flash-correct; 15: Flash-incorrect; 21: sustained correct; 22: sustained incorrect; 30: non-read. The non-zero cells contain the t-test value above and the *P* value below. The reading time of the DD children was in general higher than NSRD, except for the combination of 21–32.

	10	**11**	**12**	**20**	**21**	**22**	**23**	**30**	**31**	**32**	**33**	**40**	**41**	**42**	**43**	**44**	**50**	**51**	**52**	**53**	**60**	**61**	**62**	**63**	**70**	**71**
11				2.92 0.004																						
15																										
21				2.21 0.028						−2.38 0.019						2.64 0.025				2.41 0.024						
22																				9.35 0.003						
30																										

3.2. Results of the QEEG

The t-tests algorithm described in Section 2.5 was used to compare the EEG Z-spectra of the two groups for all leads and frequencies of the High Spectra Resolution (HSR) model. The Z-spectra values have been corrected by the age and account for EEG differences due to maturation since this is an important factor to be considered at this epoch of the life. The results are shown in Figure 1. In this comparison DD group was subtracted from the NSRD group, therefore patches in red in Figure 1 represent excess of activity in DD group regarding NSRD group and the blue patches represent leads and frequencies where the activity of DD group was significantly lower than NSRD. As it is observed, the DD children showed significant excess in delta band in the middle line (Fz, Cz and Pz), as well as Fp2 and the occipital leads bilaterally (O1 and O2). A significant excess in high theta (6–7.5 Hz) and low alpha (7.5–8.5 Hz) bands was also present in the Fz, Cz and Fp2. Fz, Cz and Pz also showed significant excess of activity in the DD group. However, a significant reduction of high alpha (11–12.5 Hz) activity was present in the DD group bilaterally in F3, C3, C4 and in P3 but more pronounced in the left leads. Additionally, significant reduction was also present in the left leads F7, F3, C3, P3 and T5.

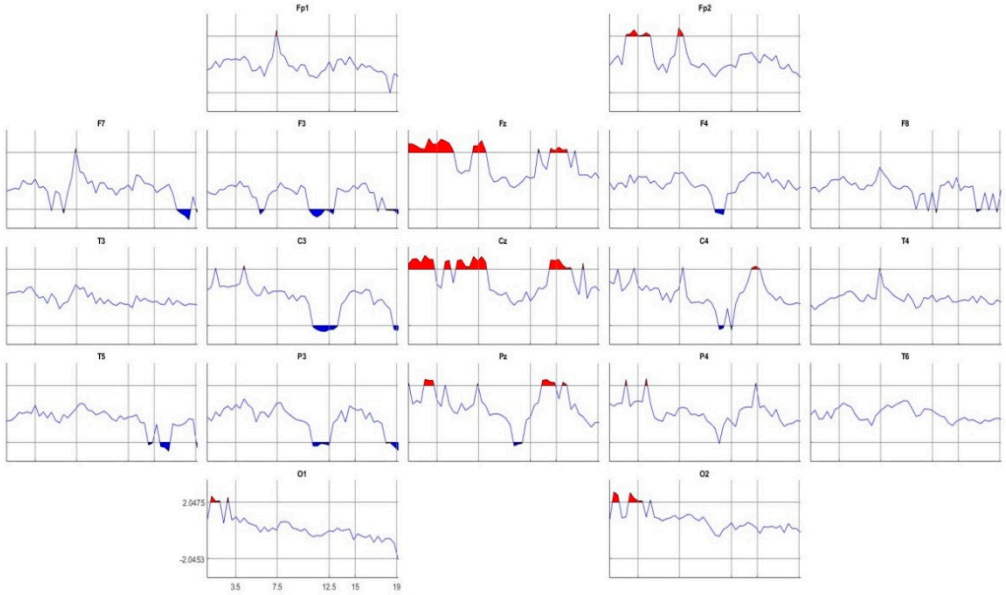

Figure 1. Results of the *t*-test between DD and NSRD groups for the Z-EEG spectra at all leads and frequencies. Main significant differences are an excess of activity of the DD group in the middle line in almost all frequency bands and a reduction of fast activity in the left fronto-parietal and temporal leads.

The *t*-tests at the sources showed a significant increase of activity of DD with respect to NSRD in Delta, low (4.29 Hz) and high theta (7.5 Hz) bands, and a significant decrease of DD with respect to NSRD in Beta band (18–19 Hz). In Delta band: bilaterally in the Calcarine sulcus, Cuneus, Precuneus, Lingual, Occipital (Superior, Middle and Inferior lobes), Fusiform and Superior Parietal; the Right Inferior Parietal, the right angular gyrus and the right Paracentral Lobule. In the low theta band: the right superior parietal and the right inferior parietal Gyrus (or lobe). In the high theta band: bilaterally the Frontal Medial Orbital and the Right Superior Medial Frontal gyri. In the Beta band:bilaterally the Calcarine sulcus, Lingual and Fusiform Inferior gyri; the Left Occipital (Superior, Medial and Inferior), Superior and Inferior Parietal, Supramarginal, Angular and Middle and Inferior Temporal (Figure 2).

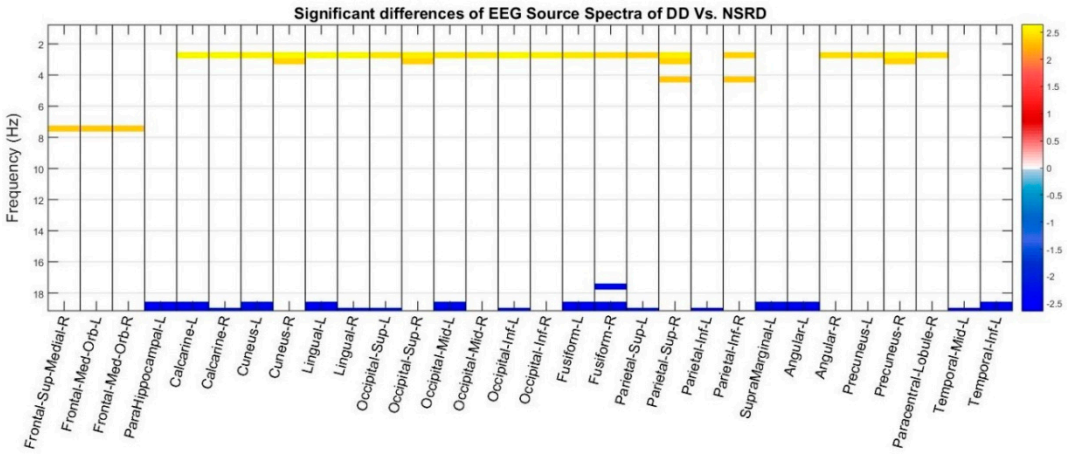

Figure 2. Significant differences of the *t* test at the sources spectra of DD vs NSRD. Red and yellow values indicate an excess of DD compared to NSRD; values in the blue scale indicates excess of NSRD compared to DD. Threshold corrected by multiple comparisons. Differences are concentrated in very narrow bands of frequencies. In general, DD have an excess of slow activity (Delta and slightly Theta) and a defect of fast activity (Beta band).

3.3. Biomarkers Results

We applied the biomarkers selection methodology to the variables of the DTRS as well as to the Z-spectra at the electrodes and at the sources separately. The discrimination power of each classification equation was measured by the robust area under the ROC curve (rAUC) and the ROC discrimination value at the 10% and 20% of False Positives.

Table 6 summarizes the variables of the anamnestic data and of DTRS selected as classifiers during the classification procedure. The second column indicates the percent of times that the variable was selected as biomarker during the random classification procedure. The last column shows the coefficient of each variable in the final classification equation. Class, comorbidity and speech therapy were selected from the anamnestic data, as the most frequent ones (more than 95%). The FSIQ, the VIQ, the age and the school attended at the time of DTRS testing also participated in the classification procedure. The variables of the DTRS that contribute the most to the classification procedure were the dysphonetic errors in the known words list. The errors that best contributed to differentiate the two groups were: the grapheme-phoneme correspondence, the insertion/omission of letters of known words and the total number of dysphonetic errors. Also, the dyseidetic errors in the known words list contribute to the classification: inversion of similar letters and the total number of dyseidetic errors. In the unknown words list the dysphonetic errors that classified the two groups were: missing double letters, grapheme-phoneme correspondence, omission of letters, grapheme exchange and the total number of dysphonetic errors. No specific dyseidetic errors were selected from the unknown words list but only the total number of dyseidetic errors. Consequently, the total number of dysphonetic and dyseidetic errors in the known and unknown words list was also selected. In contrast to the spelling test, in the reading test there were not many errors that contributed to the classification of the two groups. The most frequent error was confusion of visually similar graphemes both in flash and untimed mode together with the production of non-words in flash mode, dyseidetic errors.

Figure 3 shows a scatterplot with the classification value obtained for each subject in the sample using the final classification equation, divided by groups. For each group a boxplot with the mean and standard deviation of the individual values is presented.

Table 6. Biomarkers obtained from the classification procedure with the Clinical and Anamnestic variables (first column). The second column indicates the percent of the times the variables were selected as biomarkers during the random classification procedure. The third column is the coefficient that accompany each variable in the final classification equation. The stable area under the ROC for this equation is 0.94.

Variables	Percent	Coeff.
Anamnestic and clinical data		
Class	100	0.031413
Comorbidity	100	0.029233
Speech therapy	96.36	0.053496
Verbal Intelligent Quotient	86.57	0.025448
Age at DTRS	83.56	0.029181
School at DTRS	80.85	−0.00266
Full Scale Intelligent Quotient	78.57	0.005488
DTRS: Writing Test: Dysphonetic errors in the known words list		
Grapheme-phoneme correspondence	77.59	0.049424
Omission of letters	76.67	0.005422
Number of dysphonetic errors	76	0.016698
DTRS: Writing Test: Dyseidetic errors in the known words list		
Errors of reversal of similar letters	72.13	−0.001226
Number of dyseidetic errors	70.49	0.010814
DTRS: Writing Test: Dysphonetic errors in the unknown words list		
Missing double letters	67.86	0.000454
Accent errors	67.35	0.004261
Grapheme-phoneme correspondence	62.5	0.03555
Omission of letters	62	0.054781
Grapheme mismatch	60.38	−0.034673
Number of dysphonetic errors	59.18	0.018046
DTRS: Writing Test: Dyseidetic errors in the unknown words list		
Total dyseidetic errors	55.17	−0.009407
Total errors in the known and unknown words lists combined		
Total dysphonetic errors	54.39	0.021067
Total dyseidetic errors	52.54	−0.005514
DTRS: Reading Test: Dyseidetic errors in flash mode		
Confusion of visually similar graphemes	51.52	−0.019377
Dyseidetic non-words	50.75	0.016049
DTRS: Reading Test: Dyseidetic errors in untimed mode		
Confusion of visually similar graphemes	50.75	−0.03763

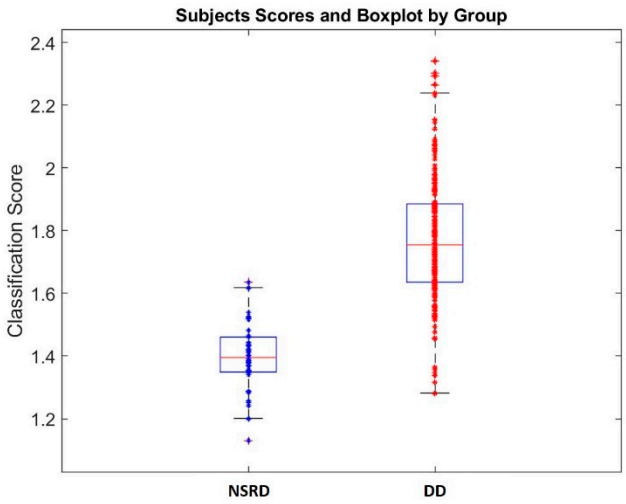

Figure 3. Scatterplot showing the individual scores obtained by the classification equation of the DTRS variables, for the subjects of the two groups NSRD (unspecific reading delay) and DD (dysphonetic dyslexics). For each group a boxplot with the mean and standard deviation of the individual values is shown.

The rAUC for the classification equation was 0.94, with a 0.87 discrimination power at the 10% of False Positive and 0.93 at the 20%. These results are shown in Figure 4.

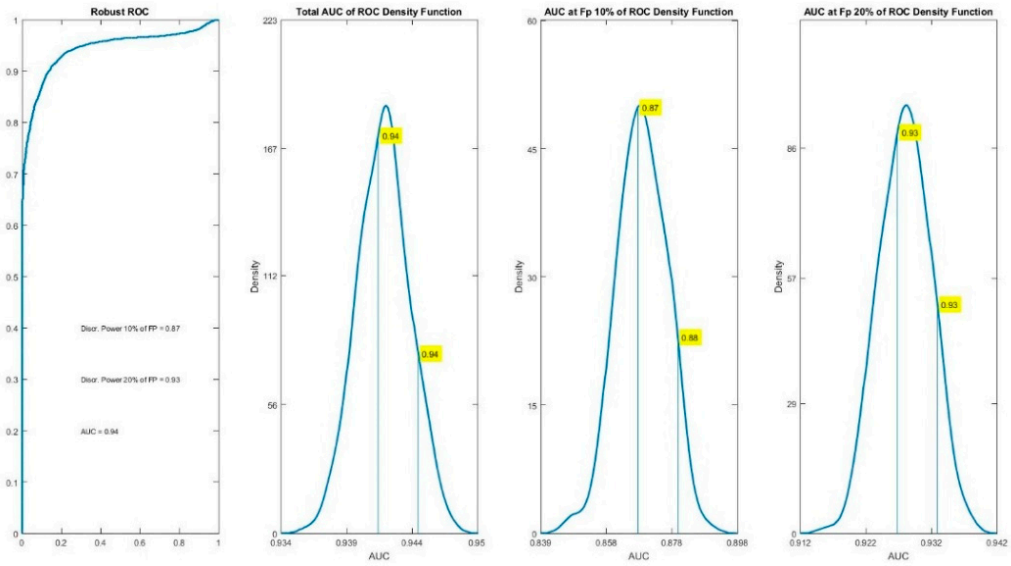

Figure 4. rAUC for the classification equation showing a value of 0.94, which indicates almost perfect sensitivity and specificity. The three panels at the right show the density functions of the total rAUC as well as the discrimination power at the 10% and 20% of False Positives, obtained by the 500 random realizations. The discrimination power at the 50% of the density function was of 0.87 for the 10% of False Positives and 0.93 at the 20% of False Positives.

Left panel in Figure 4 shows the rAUC obtained after the stable classification procedure. The other 3 panels show the distribution density of the total rAUC and the discrimination values at 10% and 20% of False Positive respectively, obtained by the robust procedure for the ROC curve. This consists in 500 random repetitions of the ROC curve calculation with random subsamples, as described in the methodology. As the rAUC, the values at the 50% of the density distributions are selected.

The stable biomarkers identification procedure was also performed with the EEG spectra both at the electrodes and at sources level. However, they did not produce high classification values as it was the case with the DTRS and clinical variables. Therefore, we do not describe them in detail. At the electrodes, the rAUC was 0.73, with a discrimination power of 0.36 at 10% and 0.51 at 20% of False Positive. The variables which participated in the classification equation were Fz and Cz in Delta band; C4 in High Alpha; and F7, Fz, and Pz in Beta band.

At the sources level, the rAUCwas 0.73, with a discrimination power of 0.24 at 10% and 0.53 at 20% of False Positive. The variables which participated in the classification equation were: in Delta band: the Left Middle Frontal lobule, the Left Middle Cingulum and the Right Hippocampus; in Alpha band: the Left Posterior Cingulum; in Beta band: the Right Superior Fronto-Orbital lobule, the Right Inferior Frontal Operculus, the Left Frontal Inferior Triangularis, the Right Middle Cingulum, the Left Posterior Cingulum, the Right Middle Occipital, the Right Heschl, and the Right Superior Temporal Pole.

4. Discussion

Statistical comparisons between DD subjects and those with NSRD have led to interesting and important results. The most significant results were found among anamnestic data and those of the DTRS. In particular, subjects with NSRD came to our observation much later than the DD subjects when they were in the last grade of primary school or the first year of secondary school (Table 2). A possible explanation of this delayed bringing to the medical doctors' attention could lie in the fact that these subjects do not make reading and spelling errors so numerous as to suspect a problem

of reading and writing. These children seem overlooked by the teachers because their reading and writing performances differ quantitatively but not qualitatively from those of normal readers and therefore they are referred to medical doctors when they are in the last grade of primary school or much worse when they are at the first grade of secondary school. In fact, these subjects have a spelling test percentage of correctly written words greater than 80. Unlike the reading difficulties present in the dyslexic readers which are often discriminative and clearly contrasting with their abilities and performances, the NSRD have a global performance usually below the norm that is associated with emotional disorders and poor motivation. In fact, the NSRD subjects had a significantly greater number of comorbidities compared to the DD subjects. The most frequent comorbidity after ADHD was the emotional disorder of anxious type. The most common type of comorbidity in the two groups, although the difference was not significant, was ADHD of inattentive type: 47% in the DD subjects and 50% in the NSRD subjects. Although ADHD and SLD are commonly considered to be a separate disorder (DSM-V American Psychiatric Association 2013) many researchers working in this field have observed that dyslexia and ADHD are closely associated. If this association is a true comorbidity or it is, instead, another neurobiological condition it is still subject of discussion and goes beyond the scope of this work.

Another data worthy of attention also comes from the analysis of reading quotients. The subjects with NSRD had a significant lower RQ, RQM and RQC than the subjects with DD. The lower reading quotients in these subjects are explained by the fact that they had a lower reading level and a higher age than the DD subjects.

This observation is also reflected in the mode of reading words in flash presentation. The NSRD subjects had a number of words read significantly more hesitantly than the DD subjects (Table 4). This modality is not typical of dyslexic subjects and in particular of DD subjects. In fact, these subjects prefer to read a word globally as instantaneous visual gestalt, rather than analytically. Their reading, because of their limited sight vocabulary is precipitous; they may guess a word from minimal clues for example from the first or last letter and the length of the word. Again, very often they do not realize the mistakes because they believe that the word they read is not part of their vocabulary. NSRD subjects, on the other hand, seem to be more aware of their difficulties and they do not rush to read a word in flash mode. Other and more numerous significant differences were observed in the second part of the DTRS, the spelling test. DD subjects made significantly more errors than NSRD subjects in both unknown and known word lists. In the list of known words, the most frequent error was the insertion/omission of letters and syllables. This error was also present even more frequently in the list of unknown words (typical error of sequencing of the DD subjects). Other errors of dysphonetic type have been found in the list of unknown words. Lack of double letters, lack of accents, correspondence grapheme/phoneme errors and similar grapheme exchange were significantly more numerous in DD subjects than NSRD. Reading times in both flash and untimed mode when analyzed individually were not significantly different between the two groups. However, when they were analyzed in relation to the complexity index, i.e., number of syllables and number of orthographic difficulties in the word, the DD subjects read much more slowly plurisyllabic words, 4 or 5 syllables, that contained 3 or 4 orthographic difficulties than the NSRD subjects. The fact that with plurisyllabic words, 6 or 7 syllables, these differences were no longer present can be explained by the reduced number of words read in the highest-grade list.

This data allows us to make general methodological and clinical remarks. The lack of significant differences between groups may depend on several reasons: an inaccurate criteria selection of clinical subjects to be examined, the test is not sufficiently demanding for the subjects to bring out differences or more often, the selected test is not appropriate or is not adequately developed to answer either the clinical questions or the model under investigation.

Since the beginning of its publication, the Boder test has received some criticisms, not mainly because of its theoretical construct and clinical acumen, but for the lack of robust normative and validation studies [71,72]. This led to conflicting results and to questioning the existence of the patterns

described by Boder. To our opinion, a limitation of the Boder test is that it was developed in the 1960s, when electronic devices were not yet available and therefore it was a paper and pencil test. The flash exposure was obtained by sliding a sheet of paper on a list of words and the classification of instantaneous gestalt reading within a second was entrusted to the experience of the examiner. Therefore, the presentation of words in flash mode was not standardized. Since visual and auditory processing during reading work in parallel, the use of both channels cannot be excluded when an unknown word is presented on paper and consequently it makes difficult to select "unknown" words for the spelling test. This subjectivity may explain the failure to distinguish the reading-spelling patterns and the contradictory results, and it may have introduced differences in the identification of subtypes. The Italian version of the Boder test that we developed in 2001 [3], which is the one used in this paper, is profoundly different from its original version: it is based on normative data built ad hoc, it is a self-paced test, it has been completely automated both in the exposure of words [73] (the words were presented in flash mode only for 250 ms and in untimed mode for 10 s.) and it differs in the recording of reading times that are missing in the original version, being a paper test. The reading and writing errors have been quantitatively and qualitatively analyzed. There is some criticism on the original version of the Boder test about lack of uniformity of its spelling test [71], on which the reading and spelling patterns are primarily based. In the Italian version, being the Italian a transparent language, the selection of words has always followed the same criteria: (a) the known words are chosen at the reading level of the subject and the unknown words are chosen at a higher grade, and (b) they are selected from the words not read or read with great difficulty. In this way we were pretty sure that the words selected for the unknown list were not in the sight vocabulary of the child, adding, therefore, consistency throughout the test.

The subtypes identified in the Boder test have been replicated by many other authors using an indirect approach [74–81]. For a comprehensive revision of this topic, see [5].

The Boder model of dyslexia [1] predicts that in the dyslexic child the normal reading process is dissociated. The normal automatic interplay of gestalt and analytic-synthetic processes is disrupted. The dyslexic child reads and spells differently from the normal reader both qualitatively and quantitatively. In our specific case, to adapt the DTRS to the characteristics of the Italian language and to respect the Boder model we needed to modify the original paper and pencil test: computerization and self-paced reading. The computerization allowed us to present words in flash mode for 250 ms. that in a previous study [73], we proved to be sufficient for a gestalt reading and to record the reading times. With self-paced action we monitor the actual intention of the child to read when pressing a button. Chiarenza et al. [82] demonstrated important electrophysiological differences between a self-paced and an externally paced reading. Even less brain activation was present during passive vision of letters.

Further evidence of the differences between these two groups of subjects comes from the QEEG. As reported by numerous studies already mentioned in the introduction, the main differences consisted of a significant power spectra excess of the DD group in the delta band in the left prefrontal, middle frontal, central, parietal, right parietal and theta power spectra excess in the prefrontal areas bilaterally, and central midline. Additionally, in the same occipital and parietal lobes except the precuneus bilaterally and the right angular gyrus, besides a theta excess, there is also a reduction of beta activity. Excess of slow waves (Delta and Theta) have been related to lower arousal, whereas excess of small beta activity indicates an alert but relaxed state [83].

While excess of delta in children with learning disabilities has been widely reported also recently [84], theta excess has not received unanimous consent. The excess of theta activity in the EEG at rest has been consistently reported in LD-NOS children [16,27,33,85–88]. Compared with children with good academic achievements, LD-NOS children had evident excess of theta activity (from 3.52 to 7.02 Hz) [86]. However, some authors who have studied this entity have not reported excess in theta activity [11,89,90] although it may be due to the composition of their samples and to the frequency of different types of pathological patterns in the extensive group of LD-NOS. Neurometric QEEG

abnormalities have been shown to be directly related to academic performance carefully documented in both reading and writing. Increased delta and/or theta power and decreased alpha power were associated with a poor educational evaluation; increased theta and/or decreased alpha were associated with mildly abnormal evaluations; and increased alpha and decreased theta were associated with good evaluations. Theta excess with alpha deficit was described as reflecting maturational lag, whereas delta excess indicated cerebral dysfunction [33].

The observation of differences of EEG source spectra between the two groups allows us to add further considerations. The first observation concerns the excess of delta and theta activity that is found in the dysphonetic subjects in a standard EEG recorded at rest, with eyes closed. This fact reinforces the hypothesis that dyslexia is not only a functional disorder, but the result of a structural disorder as reported by the studies of Galaburda [91–96] that found in the brain of 5 severe dyslexics adults the right temporal planum wider than the left in 100% of cases. In addition, a high frequency of microdysgenesis was also observed, particularly in the left frontal and temporal opercula [91,97]. This report was subsequently confirmed by Shaywitz et al. [98] who performed a series of language-based activation tasks with progressively increasing phonologic demands using fMRI in dyslexic adults. There was underactivation of the left posterior perysilvian and occipital regions (Wernicke's area, the angular gyrus and striate cortex) and overactivation to even simple phonologic task in both left anterior (inferior frontal gyrus) and right posterior perysilvian regions (see also for a review on this topic [99]). Together with the aforementioned brain areas, Wood and Flowers [100], with a factor analytic validation across 100 cases (50 normal and 50 dyslexic), using positron emission tomography have identified 43 candidate regions involved in reading and writing. The EEG sources identified with our method (Figure 2) confirm what was already found with other neuroimaging methods. To those cerebral areas already described the superior, middle and medial frontal areas show an excess of theta. A certain dysregulation of the motor areas in dyslexic subjects has long been known [101,102]. Dyslexic patients have difficulty processing both rapid and visual stimuli as well as in generating rapid bimanual motor output. Chiarenza et al. [103–105] and Chiarenza [106] recorded the brain electrical activity, called "movement-related brain potentials", during a skilled motor task that to be performed adequately, required bimanual coordination, bimanual ballistic movements, adaptive programming and learning a proper timing. The dyslexic children presented a deficit of programming movements, a deficit of visual and kinesthetic sensory processes, and a reduced capacity to evaluate their performance and correct their errors. Chiarenza [46] advanced the hypothesis that dyslexia is not only a phonological or gestalt deficit, but also a praxic disorder in which praxic abilities, such as motor programming, sequential and sensorial motor integration and evaluation processes, are required and somehow defective in dyslexia.

In addition, Chiarenza [106] has observed that dyslexic children showed a latency delay of movement-related potentials significantly different among the various cerebral areas during the same skilled motor task. Therefore, Chiarenza [106] has hypothesized that dyslexia could be the result of a timing defect that causes an integration defect and dysfunction of numerous processes hierarchically organized that occur at different levels and times. Also, Llinas [107] hypothesizes that at the base of the pathophysiology of dyslexia exists a more basic deficit of timing. This dyschronia results from a cellular dysfunction that modifies "the normal properties of neuronal circuits responsible for temporal aspects of cognition" so that the nervous system can function in a relatively normal fashion only within a temporal window. Llinas postulates that for some reason these neurons are unable to generate sharp enough ensemble oscillations at higher frequencies and reset such rhythmicity following close-interval sensory stimulation. Moreover, the dyschronia does not apply to a particular cerebral locus, but it is much wider and involves the entire brain network involved in learning and reading. Likewise, the same timing concept can be applied to the various EEG frequency bands. Different frequencies favor different types of connections and different levels of computation. In general, slow oscillations can involve many neurons in large brain areas, whereas the short time windows of fast oscillators facilitate local integration [108]. Reading, as Boder claims, requires the perfect dynamic interplay of

intact visual-gestalt and analytic-auditory function and integration of both peripheral and central processes. Therefore, the excess of delta and theta found in our dysphonetic subjects could reflect a temporal dysregulation already observed with other methodologies at various brain levels and in different cerebral areas.

This dynamic interplay of different frequencies in different brain areas confirms the idea of how the process of reading and writing occurs through a complex network in different brain areas and therefore it seems plausible that an alteration at one point in the network is inevitably reflected in other areas of the brain. A possible explanation of this temporal dysregulation could be explained as a compensatory mechanism or, alternatively, to the fact that in the dysphonetic subjects the normal automatic interplay of gestalt and analytic-synthetic processes is interrupted. The DD subjects tend to persist in the gestalt approach preferring to guess at unfamiliar words rather than employ their word-analysis skills.

Bosch-Bayard et al. [34] have given strong evidence of the validity and robustness of the biomarkers selection procedure based on the GLMNet method. GLMNet itself has also been successfully applied in different clinical situations [109–111]. In particular, the variables that had the best discriminating power were those of the DTRS and the anamnestic data, with a value of 0.94 for the stable area under the ROC curve. This very high discrimination also had a high specificity at a value of 10% of False Positives (see Figure 4). Therefore, the DTRS appears as a very useful tool for the differentiation of the DD regarding the NSRD. Among the anamnestic data, the FSIQ, VIQ and the speech therapy had a discriminating power in addition to the age and class at the time of the administration of DTRS. The FSIQ, VIQ and speech therapy had a frequency rate of 78.5, 86.5 and 96.3, respectively (see Table 6). The verbal subscales of WISCIII evaluates the quality and quantity of vocabulary and information. Due to their poor vocabulary the DD subjects scored lower than the NSRD subjects. They also had a history of speech therapy because of their obvious difficulties.

Table 6 also shows that errors in reading and spelling contributed significantly to the classification of the two groups. In the reading test, the biggest differences between the two groups were the confusion of visually similar graphemes both in flash and untimed mode and the production of non-words in flash mode.

The list of known words of the spelling test, constructed with words that are part of the subject's sight vocabulary, is intended to evaluate the child's ability to 'revisualize' the words in his sight vocabulary. The lists of unknown words, made with words that the subjects have not been able to read or have read with great difficulty, evaluate the child's ability to spell words not in his sight vocabulary. From the list of known words, mismatches of grapheme-phoneme, omission of letters, and reversal of similar letter were selected as biomarkers. From the list of unknown words, errors of accentuation, lack of double, omission of letters, exchange of similar graphemes were also selected. The DD subjects had a greater number of errors compared to NSRD subjects.

Previous studies have found that dysphonetic and dyseidetic children have almost identical profiles. Clustering techniques using neuropsychological and psychoeducational measures have yielded fairly homogeneous clusters corresponding to the proposed dysphonetic and dyseidetic subtypes [72,112–114]. Our findings indicate that there are significant differences between DD and NSRD groups at the neuropsychological level. Additionally, our classification procedure mostly selected dysphonetic errors and only two dyseidetic errors, which are present only in the reading test: confusion of visually similar graphemes both during flash and untimed mode. The minus sign of the coefficients in Table 6 indicates that subjects with NSRD had more errors of this type than DDs.

On the other hand, the EEG did not exhibit a high classification power of the two groups. The EEG spectra were analyzed both at the leads as well as at the sources in the whole frequency range of the HSR model. However, neither of the two equations obtained high discrimination power with the stable ROC technique (0.73 for the EEG spectra at the scalp and 0.73 for the spectra at the sources, see Section 3.3). These results point out that even when electrical activity between the two groups show differences, they do not clearly discriminate them with high sensitivity and specificity.

5. Conclusions

In this work we have described the clinical and neurophysiological characteristics that distinguish DD subjects from NSRD. The DTRS proved to be the one with the most discriminating power. The number and type of writing errors are those that better differentiate the two groups. The constant presence of dysphonetic and dyseidetic errors in subjects at the end of the first cycle of primary school must promptly draw the attention of teachers who must request a thorough clinical evaluation for the obvious therapeutic and prognostic implications.

Author Contributions: J.B.-B. participated in data organization and curation, algorithm programming, data processing and statistical analysis, figures and tables creation, hypothesis elaboration, paper organization and writing; V.P. participated in clinical data collection, patients' testing, databases organization, data quality control, tables creation; L.G. participated in the statistical analysis, discussions and the revision of the manuscript; P.V.-S. participated in designing the methodology, discussions and paper revision; G.A.C. is project leader and participated in clinical data collection, organization and curation, figures and tables creation, literature revision, hypothesis elaboration, provided the neuropsychiatric knowledge, paper organization and writing.

Funding: This research has been partially supported by Grant PAPIIT IA201417, DGAPA-UNAM, Mexico.

Acknowledgments: We wish to thank the two unknown reviewers for their thoughtful comments and in particular for very helpful English revision of the paper. We also wish to thank Barbara Sasselli and Igor De Marchi, the two EEG technicians for their dedication and professionalism during childrens' EEG recording.

Conflicts of Interest: The authors declare no conflict of interest.

Appendix A.

Appendix A.1. Classification of Errors of the Reading Test

Dysphonetic errors:

- Wild guesses: the word read doesn't have any correspondence with the word presented;
- Gestalt substitution: the visual structure of the word is clearly recognizable; the elements that recall the words presented are: the length of the words, the presence of the initial and final syllables, or the central syllables; sometimes the central syllables could be omitted in plurisyllabic words
- Semantic substitution: words closely related conceptually but not phonetically;
- mismatch of similar homologous grapheme or inexact grapheme;
- insertion/omission of letters of known words,
- Non-words: the word read have phonological inaccuracies, accentuation errors, or sequencing errors.

Dyseidetic errors:

- Confusion of visually similar graphemes;
- Initial fragment: words read only with the initial syllables;
- Visuo-spatial reversal of letters and syllables;
- Non-words: the word read have phonological inaccuracies, visuo-spatial reversal of letters and/or syllables.

Appendix A.2. Classification Errors of the Spelling Test

Dysphonetic errors:

- Missing Lack of double letters;
- Lack of accent
- Insertion/omission of letters

Correspondence grapheme-phoneme

- mismatch of similar graphemes;
- Good phonetic equivalent.
- Dyseidetic errors:
- Visuo-spatial reversal of syllables or letters;

References

1. Boder, E. Developmental Dyslexia: A diagnostic approach based on three typical reading-spelling patterns. *Dev. Med. Child Neurol.* **1973**, *15*, 663–687. [CrossRef] [PubMed]
2. Boder, E.; Jarrico, S. *The Boder Test of Reading-Spelling Patterns*; Grune & Stratton: New York, NY, USA, 1982.
3. Chiarenza, G.A.; Bindelli, D. Il test diretto di lettura e scrittura (DTLS): Versione computerizzata e dati normativi. *Giornale Neuropsichiatria dell'Età Evolutiva* **2001**, *21*, 163–179.
4. Luisi, A.; Ruggerini, C. *Dislessia e Disagio Pedagogico, un Approccio Interdisciplinare per la Diagnosi e L'aiuto*; Editrice TEMI: Bologna, Italy, 1997.
5. Chiarenza, G.A.; Di Pietro, S.F. La dislessia e i suoi sottotipi. Modelli clinici e risvolti applicativi nel trattamento della dislessia evolutiva. In *Dentro la Dislessia*; Sidoti, E., Ed.; Junior Edizioni: Brescia, Italy, 2014; pp. 107–132.
6. Ginn, R. An Analysis of Various Psychometric Typologies of Primary Reading Disability. Unpublished Ph.D. Thesis, University of Southern California, Los Angeles, CA, USA, 1979.
7. Naiden, N.; Basic Skills Department of the Seattle Public Schools, Washington, UK; Winger, J.; Department of Early Childhood Education, Oslo and Akershus University College of Applied Sciences, Oslo, Norway. Personal communication, 1972.
8. Nockleby, D.M.; Galbraith, G.C. Developmental dyslexia subtypes and the Boder test of reading spelling patterns. *J. Psychoeduc. Assess.* **1984**, *2*, 91–100. [CrossRef]
9. Breznitz, Z.; Meyler, A. Speed of lower-level auditory and visual processing as a basic factor in dyslexia: Electrophysiological evidence. *Brain Lang.* **2003**, *85*, 166–184. [CrossRef]
10. Žarić, G.; Fraga González, G.; Tijms, J.; Van der Molen, M.W.; Blomert, L.; Bonte, M. Cross-modal deficit in dyslexic children: Practice affects the neural timing of letter-speech sound integration. *Front. Hum. Neurosci.* **2015**, *24*, 9–369. [CrossRef]
11. Chabot, R.J.; di Michele, F.; Prichep, L.; John, E.R. The Clinical Role of Computerized EEG in the evaluation and treatment of learning and attention disorders in children and adolescents. *J. Neuropsychiatry Clin. Neurosci.* **2001**, *13*, 171–186. [CrossRef] [PubMed]
12. Hughes, J.R. Electroencephalographic and neurophysiological studies in dyslexia. In *Dyslexia: An Appraisal of Current Knowledge*; Benton, A., Peal, D., Eds.; Oxford University Press: New York, NY, USA, 1978; pp. 207–240.
13. Byring, R.; Jarvilehto, T. Auditory and visual evoked potentials of schoolboys with spelling disabilities. *Dev. Med. Child Neurol.* **1985**, *27*, 141–148. [CrossRef] [PubMed]
14. Conners, C.K. Critical review of electroencephalographic and neurophysiologic studies in dyslexia. In *Dyslexia: An Appraisal of Current Knowledge*; Benton, A., Peal, D., Eds.; Oxford University Press: New York, NY, USA, 1978; pp. 251–261.
15. Becker, J.; Velasco, M.; Harmony, T. Electroencephalographic characteristics of children with learning disabilities. *Clin. Electroencephalogr.* **1987**, *18*, 93–101. [PubMed]
16. Alvarez, A.; Perez-Avalo, M.C.; Morenza, L. Neuropsychological assessment of learning-disorder children with paroxysmal EEG activity. *New Issues Neurosci.* **1992**, *4*, 40–50.
17. Koyama, M.S.; Di Martino, A.; Zuo, X.N.; Kelly, C.; Mennes, M.; Jutagir, D.R.; Castellanos, F.X.; Milham, M.P. Resting-state functional connectivity indexes reading competence in children and adults. *J. Neurosci.* **2011**, *31*, 8617–8624.
18. Koyama, M.S.; Di Martino, A.; Kelly, C.; Jutagir, D.R.; Sunshine, J.; Schwartz, S.J.; Castellanos, F.X.; Milham, M.P. Cortical signatures of dyslexia and remediation: An intrinsic functional connectivity approach. *PLoS ONE* **2013**, *8*, e55454.
19. Zhang, M.; Li, J.; Chen, C.; Xue, G.; Lu, Z.; Mei, L.; Xue, H.; Xue, F.; He, Q.; Chen, C.; et al. Resting-state functional connectivity and reading abilities in first and second languages. *NeuroImage* **2014**, *84*, 546–553.

20. Hoeft, F.; McCandliss, B.D.; Black, J.M.; Gantman, A.; Zakerani, N.; Hulme, C.; Lyytinen, H.; Whitfield-Gabrieli, S.; Glover, G.H.; Reiss, A.L.; et al. Neural systems predicting long-term outcome in dyslexia. *Proc. Natl. Acad. Sci. USA* **2011**, *108*, 361–368. [CrossRef] [PubMed]
21. Niogi, S.N.; McCandliss, B.D. Left lateralized white matter microstructure accounts for individual differences in reading ability and disability. *Neuropsychologia* **2006**, *44*, 2178–2188. [CrossRef] [PubMed]
22. Vandermosten, M.; Boets, B.; Wouters, J.; Ghesquière, P. A qualitative and quantitative review of diffusion tensor imaging studies in reading and dyslexia. *Neurosci. Biobehav. Rev.* **2012**, *36*, 1532–1552. [CrossRef] [PubMed]
23. Liu, K.; Shi, L.; Chen, F.; Waye, M.M.; Lim, C.K.; Cheng, P.W.; Luk, S.S.; Mok, V.C.; Chu, W.C.; Wang, D. Altered topological organization of brain structural network in Chinese children with developmental dyslexia. *Neurosci. Lett.* **2015**, *589*, 169–175. [CrossRef] [PubMed]
24. Richards, T.L.; Grabowski, T.J.; Boord, P.; Yagle, K.; Askren, M.; Mestre, Z.; Robinson, P.; Welker, O.; Gulliford, D.; Nagy, W.; et al. Contrasting brain patterns of writing-related DTI parameters, fMRI connectivity, and DTI–fMRI connectivity correlations in children with and without dysgraphia or dyslexia. *Neuroimage Clin.* **2015**, *8*, 408–421. [CrossRef] [PubMed]
25. Schurz, M.; Wimmer, H.; Richlan, F.; Ludersdorfer, P.; Klackl, J.; Kronbichler, M. Resting state and task-based functional brain connectivity in developmental dyslexia. *Cereb. Cortex* **2014**, *25*, 3502–3514. [CrossRef] [PubMed]
26. Van der Mark, S.; Klaver, P.; Bucher, K.; Maurer, U.; Schulz, E.; Brem, S.; Martin, E.; Brandeis, D. The left occipitotemporal system in reading: Disruption of focal fMRI connectivity to left inferior frontal and inferior parietal language areas in children with dyslexia. *Neuroimage* **2011**, *54*, 2426–2436. [CrossRef] [PubMed]
27. John, E.R.; Prichep, L.S.; Ahn, H.; Easton, P.; Fridman, J.; Kaye, H. Neurometric evaluation of cognitive dysfunctions and neurological disorders in children. *Prog. Neurobiol.* **1983**, *21*, 239–290. [CrossRef]
28. Duffy, F.H.; Denckla, M.B.; Bartels, P.H.; Sandini, G.; Kiessling, L.S. Dyslexia: Automated diagnosis by computerized classification of brain electrical activity. *Ann. Neurol.* **1980**, *7*, 421–428. [CrossRef] [PubMed]
29. John, E.R. Neurometric evaluation of brain function related to learning disorders. *Acta Neurol. Scand.* **1981**, *64* (Suppl. S89), 87–100. [CrossRef]
30. Marosi, E.; Harmony, T.; Sánchez, L.; Becker, J.; Bernal, J.; Reyes, A.; Díaz de Léon, A.E.; Rodríguez, M. Maturation of the coherence of EEG activity in normal and learning-disabled children. *Electroencephalogr. Clin. Neurophysiol.* **1992**, *83*, 350–357. [CrossRef]
31. Marosi, E.; Harmony, T.; Reyes, A.; Bernal, J.; Fernández, T.; Guerrero, V.; Rodríguez, M.; Silva, J.; Yáñez, G.; Rodríguez, H. A follow-up study of EEG coherence in children with different pedagogical evaluations. *Int. J. Psychophysiol.* **1997**, *25*, 227–235. [CrossRef]
32. John, E.R.; Prichep, L.S. Principles of neurometrics and neurometric analysis of EEG and evoked potentials. In *EEG: Basic Principles, Clinical Applications and Related Fields*; Niedermeyer, E., Lopes Da Silva, F., Eds.; Williams and Wilkins: Baltimore, MD, USA, 1993; pp. 989–1003.
33. Harmony, T.; Hinojosa, G.; Marosi, E.; Becker, J.; Rodriguez, M.; Reyes, A.; Rocha, C. Correlation between EEG spectral parameters and an educational evaluation. *Int. J. Neurosci.* **1990**, *54*, 147–155. [CrossRef] [PubMed]
34. Bosch-Bayard, J.; Galán-García, L.; Fernandez, T.; Biscay Lirio, R.; Roca-Stappung, M.; Ricardo-Garcell, J.; Harmony, T.; Valdes-Sosa, P. Stable sparse classifiers identify QEEG signatures that predict learning disabilities (NOS) severity. *Front. Neurosci.* **2018**, *11*, 749. [CrossRef] [PubMed]
35. Roca-Stappung, M.; Fernandez, T.; Bosch-Bayard, J.; Harmony, T.; Ricardo-Garcell, J. Electroencephalographic characterization of subgroups of children with learning disorders. *PLoS ONE* **2017**, *12*, e0179556. [CrossRef] [PubMed]
36. Flynn, J.; Deering, W. Subtypes of dyslexia: Investigation of Boder's system using quantitative neurophysiology. *Dev. Med. Child Neurol.* **1989**, *31*, 215–223. [CrossRef] [PubMed]
37. Flynn, J.M.; Deering, W.; Goldstein, M.; Rahbar, M.H. Electrophysiological correlates of dyslexic subtypes. *J. Learn. Disabil.* **1992**, *28*, 133–141. [CrossRef] [PubMed]
38. Casarotto, S.; Ricciardi, E.; Sani, L.; Guazzelli, M.; Pietrini, P.; Chiarenza, G.A. Single-letter reading elicits a different spatio-temporal modulation of brain activity in dyslexic children as compared to healthy controls. *Neuroimage* **2007**, *36* (Suppl. S1), 171.

39. Chiarenza, G.A. Normal and abnormal reading processes in children. Neuropsychophysiological studies. In *Handbook of Clinical QEEG and Neurotherapy*; Thomas, F.C., John, A.F., Eds.; Routledg: New York, NY, USA, 2017; Volume 10017, pp. 235–249.
40. Velikova, S.; Chiarenza, G.A. EEG correlates of clinical subtypes of developmental dyslexia: Independent Component Analysis study. *Int. J. Psychophysiol.* **2012**, *3*, 322. [CrossRef]
41. De Sonneville, L.M. *Handbook Amsterdam Neuropsychological Tasks*; Boom Test Publisher: Amsterdam, The Netherlands, 2014.
42. *Diagnostic and Statistical Manual of Mental Disorders*, 5th ed.; American Psychiatric Association: Arlington, VA, USA, 2013.
43. Cornoldi, C.; Colpo, G. *Prove di Lettura MT-2 per la Scuola Primaria*; Organizzazioni Speciali: Firenze, Italy, 2011.
44. Cornoldi, C.; Colpo, G. *Nuove Prove di Lettura MT per la Scuola Secondaria di I Grado*; Organizzazioni Speciali: Firenze, Italy, 2012.
45. Sartori, G.; Job, R.; Tressoldi, P.E. *Batteria per la Valutazione Della Dislessia e Disortografia Evolutiva. DDE-2*; Organizzazioni Speciali: Firenze, Italy, 2007.
46. Chiarenza, G.A. *Test Diretto di Lettura e Scrittura, DTLS (Seconda edizione)*; Centro Internazionale Disturbi di Apprendimento, Attenzione, Iperattività (CIDAAI): Milano, Italy, 2010.
47. Cornoldi, C.; Lucangeli, D.; Bellina, M. *Test AC-MT 6-11: Test di Valutazione Delle Abilità di Calcolo*; Erickson: Trento, Italy, 2002.
48. Cornoldi, C.; Cazzola, C. *AC-MT 11-14: Test di Valutazione Delle Abilità di Calcolo e Problem Solving Dagli 11 ai 14 Anni*; Erickson: Trento, Italy, 2003.
49. Biancardi, A.; Morioni, E.; Pieretti, E. *BDE, Batteria per la Discalculia Evolutiva*; Omega: Torino, Italy, 2004.
50. Di Brina, C.; Rossini, G. *BHK Scala Sintetica per la Valutazione Della Scrittura in Età Evolutiva*; Erickson: Trento, Italy, 2011.
51. Tressoldi, P.; Cornoldi, C.; Re, A.M. *BVSCO-2: Batteria per la Valutazione della Scrittura e della Competenza Ortografica-2*; Giunti OS: Firenze, Italy, 2012.
52. Pascual-Marqui, R.D.; Valdes-Sosa, P.A.; Alvarez-Amador, A. A parametric model for multichannel EEG spectra. *Int. J. Neurosci.* **1998**, *40*, 89–99. [CrossRef]
53. Szava, S.; Valdes, P.; Biscay, R.; Galan, L.; Bosch, J.; Clark, I.; Jimenez, J.C. High resolution quantitative EEG analysis. *Brain Topogr. Spring* **1993**, *6*, 211–219. [CrossRef]
54. Valdes-Sosa, P.; Biscay-Lirio, R.; Galán-García, L.; Bosch-Bayard, J.; Szava, S.; Virues-Alba, T. High Resolution Spectral EEG norms for topography. *Brain Topogr.* **1990**, *3*, 281–282.
55. John, E.R.; Ahn, H.; Prichep, L.S.; Trepetin, M.; Brown, D.; Kaye, H. Developmental equations for the electroencephalogram. *Science* **1980**, *210*, 1255–1258. [CrossRef] [PubMed]
56. Gasser, T.; Bacher, P.; Mochs, J. Transformation towards the normal distribution of broadband spectral parameters of the EEG. *EEG Clin. Neurophysiol.* **1982**, *53*, 119–124. [CrossRef]
57. John, E.R.; Prichep, L.S.; Friedman, J.; Easton, P. Neurometrics: Computer-assisted differential diagnosis of brain dysfunctions. *Science* **1988**, *293*, 162–169. [CrossRef]
58. Kondacs, A.; Szabo, M. Long-term intra-individual variability of the background EEG in normals. *Clin. Neurophysiol.* **1999**, *110*, 1708–1716. [CrossRef]
59. Bosch-Bayard, J.; Valdes-Sosa, P.; Virues-Alba, T.; Aubert-Vazquez, E.; John, E.R.; Harmony, T.; Riera-Diaz, J.; Trujillo-Barreto, N. 3D statistical parametric mapping of EEG source spectra by means of variable resolution electromagnetic tomography (VARETA). *Clin. Electroencephalogr.* **2001**, *32*, 47–61. [CrossRef] [PubMed]
60. Riera, J.J.; Fuentes, M.E. Electric lead field for a piecewise homogeneous volume conductor model of the head. *IEEE Trans. Biomed. Eng.* **1998**, *45*, 746–753. [CrossRef] [PubMed]
61. Evans, A.C.; Collins, D.L.; Mills, S.R.; Brown, E.D.; Kelly, R.L.; Peters, T.M. 3D Statistical Neuroanatomical Models from 305 MRI Volumes. In Proceedings of the IEEE Nuclear Science Symposium and Medical Imaging Conference, San Francisco, CA, USA, 31 October–6 November 1993; Volume 95, pp. 1813–1817.
62. Hernandez, J.L.; Biscay, R.; Virues, T.; Szava, S.; Bosch, J.; Riquenes, A.; Clark, I. A global scale factor in brain topography. *Int. J. Neurosci.* **1994**, *76*, 267–278. [CrossRef] [PubMed]
63. Mulert, C.; Pogarell, O.; Juckel, G.; Rujescu, D.; Giegling, I.; Rupp, D.; Mavrogiorgou, P.; Bussfeld, P.; Gallinat, J.; Möller, H.J.; et al. The neural basis of the P300 potential: Focus on the time-course of the underlying cortical generators. *Eur. Arch. Psychiatry Clin. Neurosci.* **2004**, *254*, 190–198. [CrossRef] [PubMed]

64. Bolwig, T.G.; Hansen, E.S.; Hansen, A.; Merkin, H.; Prichep, L.S. Toward a better understanding of the pathophysiology of OCD SSRI responder: QEEG source localization. *Acta Psychiatr. Scand.* **2007**, *115*, 237–242. [CrossRef] [PubMed]
65. Zumsteg, D.; Wennberg, R.A.; Treyer, V.; Buck, A.; Wieser, H.G. H2(15)O or 13NH3 PET and electromagnetic tomography (LORETA) during partial status epilepticus. *Neurology* **2005**, *65*, 1657–1660. [CrossRef] [PubMed]
66. Prichep, L.S.; John, E.R.; Tom, M.L. Localization of deep white matter lymphoma using VARETA—A case study. *Clin. EEG* **2001**, *32*, 62–66. [CrossRef]
67. Corsi-Cabrera, M.; Figueredo-Rodríguez, P.; del Río-Portilla, Y.; Sánchez-Romero, J.; Galán, L.; Bosch-Bayard, J. Enhanced fronto-parietal synchronized activation during the wake-sleep transition in patients with primary insomnia. *Sleep* **2012**, *35*, 501–511. [CrossRef] [PubMed]
68. Evans, A.C.; Collins, D.L.; Neelin, P.; MacDonald, D.; Kamber, M.; Marrett, T.S. Three-Dimensional correlative imaging: Applications in human brain mapping. In *Functional Neuroimaging: Technical Foundations*; Thatcher, R., Hallet, M., Zeffiro, T., John, E.R., Huerta, M., Eds.; Academic Press: New York, NY, USA, 1994; pp. 145–161.
69. Worsley, K.J.; Marrett, S.; Neelin, P.; Evans, A.C. A unified statistical approach for determining significant signals in location and scale space images of cerebral activation. In *Quantification of Brain Function Using PET*; Myers, R., Cunningham, V.G., Bailey, D.L., Jones, T., Eds.; Academic Press: San Diego, CA USA, 1995; pp. 327–333.
70. Friedman, J.; Hastie, T.; Tibshirani, R. Regularization paths for generalized linear models via coordinate descent. *J. Stat. Softw.* **2008**, *33*, 1–22. [CrossRef]
71. Reynolds, C.R. Clinical Acumen but Psychometric Naivete in Neuropsychological Assessment of Educational Disorders. *Arch. Clin. Neupsychol.* **1986**, *1*, 121–137. [CrossRef]
72. Howes N., L.; Bigler, E.D.; Lawson, J.S.; Burlingame, G.M. Reading Disability Subtypes and the Test of Memory and Learning. *Arch. Clin. Neuropsychol.* **1999**, *14*, 317–339. [CrossRef] [PubMed]
73. Chiarenza, G.A.; Coati, P.; Cucci, M. Development of gestalt-reading processes in children: Assessment using the Boder test. *Acta Paedopsychiatr.* **1994**, *56*, 193–197. [PubMed]
74. Kinsbourne, M.; Warrington, E. Developmental factors in reading and writing backwardness. *Br. J. Psychol.* **1963**, *54*, 154–156. [CrossRef]
75. Ingram, T.; Mason, A.; Blackburn, I. A retrospective study of 82 children with reading disability. *Dev. Med. Child Neurol.* **1970**, *12*, 271–281. [CrossRef] [PubMed]
76. Coltheart, M.; Curtis, B.; Atkins, P.; Haller, M. Models of reading aloud: Dual route and parallel-distributed-processing approaches. *Psychol. Rev.* **1993**, *100*, 589–608. [CrossRef]
77. Rourke, B.P.; Finlayson, M.A. Neuropsychological significance of variations in patterns of academic performance: Verbal and visual-spatial abilities. *J. Abnorm. Child Psychol.* **1978**, *6*, 121–133. [CrossRef] [PubMed]
78. Seymour, P.H. Individual cognitive analysis of competent and impaired reading. *Br. J. Psychol.* **1987**, *78*, 483–506. [CrossRef] [PubMed]
79. Bakker, D.J. Hemispheric differences and reading strategies: Two dyslexias? *Bull. Orton Soc.* **1979**, *29*, 84–100. [CrossRef]
80. Bakker, D.J. *Neuropsychological Treatment of Dyslexia*; Oxford University Press: New York, NY, USA, 1990.
81. Snowling, M.J. Dyslexia: A language learning impairment. *J. Br. Acad.* **2014**, *2*, 43–58. [CrossRef]
82. Chiarenza, G.A.; Olgiati, P.; Trevisan, C.; De Marchi, I.; Casarotto, S. Reading aloud: A psychophysiological investigation in children. *Neuropsychologia* **2013**, *51*, 425–436. [CrossRef] [PubMed]
83. Jena, S.P.K. *Learning Disability: Theory to Practice*; SAGE Publishing: New Delhi, India, 2013.
84. Penolazzi, B.; Spironelli, C.; Angrilli, A. Delta EEG activity as a marker of dysfunctional linguistic processing in developmental dyslexia. *Psychophysiology* **2008**, *45*, 1025–1033. [CrossRef] [PubMed]
85. Colon, E.J.; Notermas, S.L.; de Weerd, J.P.; Kap, J. The discriminating role of EEG power spectra in dyslexic children. *J. Neurol.* **1979**, *221*, 257–262. [CrossRef] [PubMed]
86. Fernández, T.; Harmony, T.; Fernández-Bouzas, A.; Silva, J.; Herrera, W.; Santiago-Rodríguez, E.; Sánchez, L. Sources of EEG activity in learning disabled children. *Clin. Electroencephalogr.* **2002**, *33*, 160–164. [CrossRef] [PubMed]
87. Jäncke, L.; Alahmadi, N. Resting State EEG in Children with Learning Disabilities: An Independent Component Analysis Approach. *Clin. EEG Neurosci.* **2016**, *47*, 24–36. [CrossRef] [PubMed]

88. Mechelse, K.; Gemund, J.J.; Nije, J.; Burg, L.; Laurs, J. Visual and quantitative analysis of EEGs of school children, children, and school children with specific reading disability. *Electroencephalogr. Clin. Neurophysiol.* **1975**, *39*, 106–108.
89. Byring, R.; Salmi, T.K.; Sainio, K.O.; Orn, H.P. EEG in children with spelling disabilities. *Electroencephalogr. Clin. Neurophysiol.* **1991**, *79*, 247–255. [CrossRef]
90. Fonseca, L.C.; Tedrus, G.M.; Chiodi, M.G.; Cerqueira, J.N.; Tonelotto, J.M. Quantitative EEG in children with learning disabilities: Analysis of band power. *Arq. Neuropsiquiatr.* **2006**, *64*, 376–381. [CrossRef] [PubMed]
91. Galaburda, A.M. The pathogenesis of childhood dyslexia. *Res. Pub. Assoc. Res. Nerv. Ment. Dis.* **1988**, *66*, 127–138.
92. Galaburda, A.M. Neurology of developmental dyslexia. *Curr. Opin. Neurol. Neurosurg.* **1992**, *5*, 7176. [CrossRef]
93. Galaburda, A.M. Neuroanatomic basis of developmental dyslexia. *Neurol. Clin. N. Am.* **1993**, *11*, 161–173. [CrossRef]
94. Galaburda, A.M. Neurology of developmental dyslexia. *Curr. Opin. Neurobiol.* **1993**, *3*, 237–242. [CrossRef]
95. Galaburda, A.M. The planum temporale (editorial). *Arch. Neurol.* **1993**, *50*, 457. [CrossRef] [PubMed]
96. Galaburda, A.M. Developmental dyslexia and animal studies: At the interface between cognition and neurology. *Cognition* **1994**, *50*, 133–149. [CrossRef]
97. Hunphreys, P.; Kaufmann, W.E.; Galaburda, A.M. Developmental dyslexia in women: Neuropathological findings in three patients. *Ann. Neurol.* **1990**, *28*, 727–738. [CrossRef] [PubMed]
98. Shaywitz, S.E.; Shaywitz, B.A.; Pugh, K.R.; Fulbright, R.K.; Constable, R.T.; Mencl, W.R.; Shankweiler, D.P.; Liberman, A.M.; Skudlarski, P.; Fletcher, J.M.; et al. Functional disruption in the organization of the brain for reading in dyslexia. *Proc. Natl. Acad. Sci. USA* **1998**, *95*, 2636–2641. [CrossRef] [PubMed]
99. Filipek, P.A.; Pennington, B.F.; Simon, J.H.; Filley, C.M.; DeFries, J.C. Structural and functional neuroanatomy disorder. In *Reading and Attention Disorders*; Duane, D.D., Ed.; York Press Inc.: Baltimore, MD, USA, 1999; pp. 43–59.
100. Wood, F.B.; Flowers, D.L. Functional neuroanatomy of dyslexic subtypes. In *Reading and Attention Disorders. Neurobiological Correlates*; Duane, D.D., Ed.; York Press Inc.: Baltimore, MD, USA, 1999; pp. 129–160.
101. Wolff, P.H.; Melngailis, I.; Kotwica, K. Impaired motor timing control in specific reading retardation. *Neuropsychologia* **1984**, *22*, 587–600. [CrossRef]
102. Wolff, P.H.; Michel, G.; Ovrut, M. The timing of syllables repetitions in developmental dyslexia. *J. Speech Hear. Res.* **1990**, *33*, 281. [CrossRef] [PubMed]
103. Chiarenza, G.A.; Papakostopoulos, D.; Grioni, A.G.; Tengattini, M.B.; Mascellani, P.; Guareschi Cazzullo, A. Movement-related brain macropotentials during a motor perceptual task in dyslexic-dysgraphic children. In *Cerebral Psychophysiology: Studies in Event-Related Potentials (EEG Suppl. 38)*; McCallum, W.C., Zappoli, R., Denoth, F., Eds.; Elsevier Science Publisher: Amsterdam, The Netherlands, 1986; pp. 489–491.
104. Chiarenza, G.A.; Papakostopoulos, D.; Guareschi Cazzullo, A.; Giordana, F.; Giammari Aldè, G. Movement related brain macropotentials during skilled performance task in children with learning disabilities. In *Clinical Application of Cerebral Evoked Potentials in Pediatric Medicine*; Chiarenza, G.A., Papakostopoulos, D., Eds.; Excerpta Medica: Amsterdam, The Netherlands, 1982; pp. 259–292.
105. Chiarenza, G.A.; Papakostopoulos, D.; Guareschi Cazzullo, A.; Giordana, F.; Giammari Aldè, G. Movement related brain macropotentials (MRBMs) and their relationship with the accuracy of skilled performance in normal and learning disabled children. In *Event Related Potentials in Children. Basic Concepts and Clinical Applications*; Rothenberger, A., Ed.; Elsevier Biomedical Press: Amsterdam, The Netherlands, 1982; pp. 243–256.
106. Chiarenza, G.A. Motor-perceptual function in children with developmental reading disorders: Neuropsychophysiological analysis. *J. Learn. Disabil.* **1990**, *23*, 375–385. [CrossRef] [PubMed]
107. Llinas, R. Is dyslexia a dyschronia? *Ann. N. Y. Acad. Sci.* **1993**, *682*, 48–56. [CrossRef] [PubMed]
108. Buzsáki, G. *Rhythms of the Brain*; Oxford University Press: New York, NY, USA, 2006; pp. 1–448.
109. Casanova, R.; Whitlow, C.T.; Wagner, B.; Williamson, J.; Shumaker, S.A.; Maldjian, J.A.; Espeland, M.A. High Dimensional Classification of Structural MRI Alzheimer's Disease Data Based on Large Scale Regularization. *Front. Neuroinform.* **2011**, *5*, 22. [CrossRef] [PubMed]
110. Chiarenza, G.A.; Villa, S.; Galan, L.; Valdes-Sosa, P.; Bosch-Bayard, J. Junior temperament character inventory together with quantitative EEG discriminate children with attention deficit hyperactivity disorder combined

subtype from children with attention deficit hyperactivity disorder combined subtype plus oppositional defiant disorder. *Int. J. Psychophysiol.* **2018**, *130*, 9–20. [PubMed]

111. Hernandez-Gonzales, G.; Bringas-Vega, M.L.; Galán-Garcia, L.; Bosch-Bayard, J.; Lorenzo-Ceballos, Y.; Melie-Garcia, L.; Valdes-Urrutia, L.; Cobas-Ruiz, M.; Valdes-Sosa, P.A. Multimodal quantitative neuroimaging databases and methods: The Cuban Human Brain Mapping Project. *Clin. EEG Neurosci.* **2011**, *42*, 149–159. [CrossRef] [PubMed]
112. McIntosh, D.E.; Gridley, B.E. Differential ability scales: Profiles of learning-disabled subtypes. *Psychol. Sch.* **1993**, *30*, 11–24. [CrossRef]
113. Swanson, H.L.; Cochran, K.F.; Ewers, C.A. Can learning disabilities be determined from working memory performance? *J. Learn. Disabil.* **1990**, *23*, 59–67. [CrossRef] [PubMed]
114. Watson, C.; Willows, D.M. Information-processing patterns in specific reading disability. *J. Learn. Disabil.* **1995**, *28*, 216–231. [CrossRef] [PubMed]